

# Targeted jumps by salticid spiders (Araneae: Salticidae: *Phidippus*)<sup>1</sup>

David Edwin Hill<sup>2</sup>

<sup>1</sup> All contents of this paper including illustrations are released for public use under a Creative Commons Attribution 3.0 Unported License

<sup>2</sup> 213 Wild Horse Creek Drive, Simpsonville, South Carolina 29680 USA, email platycryptus@yahoo.com

---

## Preface

This project began in 1978–1979 as a modest effort to measure the accuracy of jumps executed by salticid spiders. At that time, computing power was neither as accessible, nor as powerful, as it is today. Originally all photographs were measured by hand and the data was processed with a programmable calculator, one jump at a time. Initial measurements were based on graphical estimation of the starting point for each trajectory. With the later advent of personal computers, all measurements were redone from the original photographs, in order to calculate the starting point as depicted in this paper. Considering the simplicity of the subject, this work was very time-consuming. Although it is quite easy to observe the remarkable jumps of these spiders, at the time that this work was completed the relative sophistication of these small machines with respect to the processing of information was not fully appreciated. With the advent of the computer age, we have a new appreciation for miniaturization. It now appears more obvious to us that the small size of these creatures does not deter from their obvious ability to complete accurate jumps toward prey and other objectives, based on visual information that they have collected with their sophisticated visual systems. Version 7 of this paper represented a substantial revision. Topics that received only brief mention in previous versions, such as pitch and roll, were added. Many more illustrations were also added to give the reader a better understanding of salticid ballistic flight and the devices that make this possible. Version 9 includes an improved description of dragline ascent after capture of large prey, based on many recent observations of prey capture by *Phidippus princeps* in South Carolina. The present version has been produced primarily to make this work available as a number of PECKHAMIA.

## 1. Summary

Jumping spiders (adult female *Phidippus princeps* Peckham & Peckham 1883) were found to calibrate both the magnitude and the direction of their take off velocity relative to target (position or prey) direction in order to attain the required range of a jump. They jumped further above, and faster toward, more distant targets, or targets in a more horizontal direction. These results were produced from a variety of starting positions, including "right side up" and "upside down" starting positions. Significant backward pitch accompanied launch in most cases. This pitch was reversed by dragline braking toward the end of longer jumps. Spiders also used roll to move from a sideways to a horizontal orientation when jumping from a vertical surface.

## 2. Introduction

Salticid spiders are capable of executing accurate jumps that can exceed 10 cm in trajectory to capture distant or flying prey, including araneid spiders resting in their webs (Robinson and Valerio 1977). Active salticids also jump to attain target positions when they navigate through vegetation or on a surface (Hill 1977a, 1978, 2010). Since the landmark study of Parry and Brown (1959b), which focused on the mechanism of acceleration through hydraulic extension of legs IV by *Sitticus*, the jumps of these jumping spiders have received little study. Hill (1978, 2006a, 2010) has provided several demonstrations of the use of gravity by these spiders, and in particular demonstrated how they evaluated the attainable range of prey by the direction of that prey relative to gravity.

Parry and Brown (1959b) used multiple image photography to measure a take-off velocity of *Sitticus* between 64 and 79 cm/sec, close to the range of velocities observed in the present study of *Phidippus*. As

can be seen by comparison with photographs presented here, the photographs of *Sitticus* published with that study appear to depict spiders that were careening out of control during flight! That study focused primarily on calculation of forces (torques) involved in leg extension and acceleration of the jumping spider, as an extension of earlier work on spider hydraulics (Parry and Brown 1959a). Through this Parry and Brown were able to demonstrate that hydraulic extension of legs IV could power the jumps of *Sitticus pubescens*. Related biomechanics will be reviewed in more detail below.

The present study focused on the ability of these spiders to adjust take off velocity (both magnitude and direction relative to gravity and prey) to accurately target their prey or positional objectives through ballistic flight. At the same time, key dynamics related to ballistic flight, braking, and movement of the spider during flight were examined as revealed by multiple flash photography.

### 3. Materials and methods

For this study, adult female *Phidippus princeps* were reared from immatures captured in the vicinity of Ithaca, New York (Figure 1).



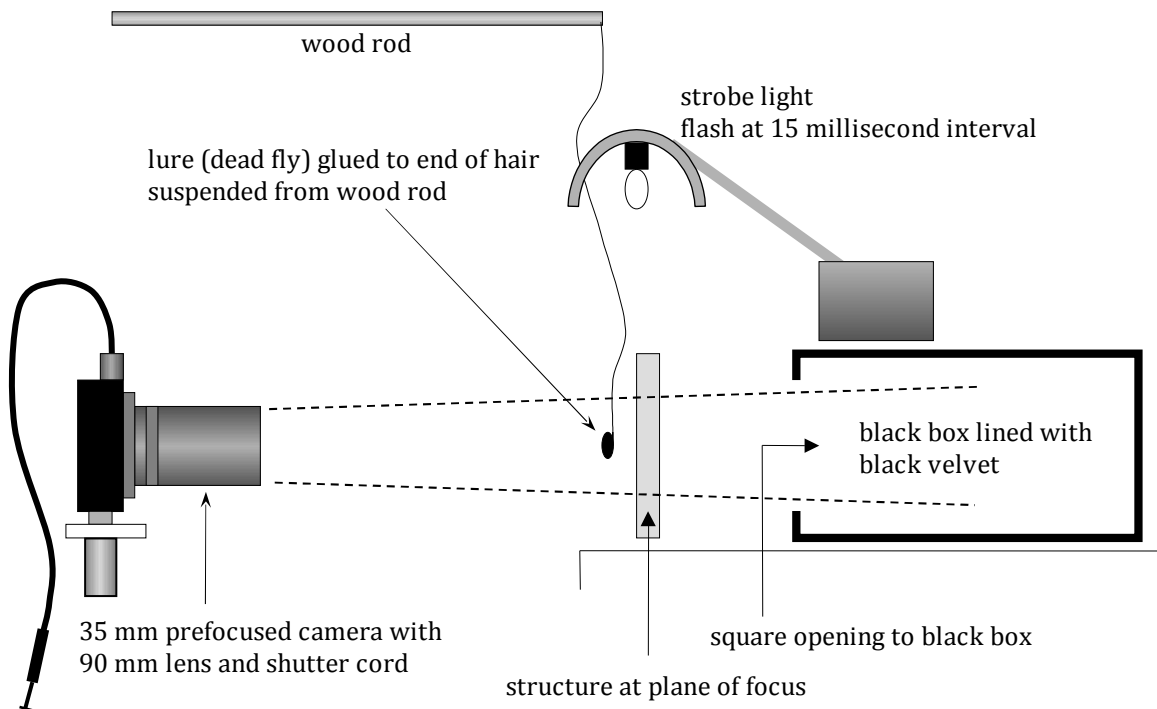
Figure 1. 1, Capture of a large fly by an adult female *Phidippus princeps* from the vicinity of Ithaca (Tompkins County), New York. 2–5, Frames from video clips of feeding adult female *P. princeps* from Greenville County, South Carolina. 2, Feeding on a captured brachyceran fly. 3, Feeding on a larger spider. 4–5, Two successive views of feeding on a small spider, before (4) and after (5) execution of a turn *in place* to face an object of interest. Note the lack of stepping movements during this turn. The pedipalps can be moved to alternately conceal and expose the iridescent green chelicerae.



*Phidippus* is a diverse genus of active and versatile predators that are attracted to both flying and sedentary prey. *P. princeps* are often abundant in transitional habitats (woodland borders near prairie) in the eastern part of the United States. They prey on a variety of insects including leafhoppers, moths, grasshoppers, and flies. They also prey on other spiders, including *Phidippus*. *P. princeps* was selected for this study because, like *P. clarus* and *P. pulcherrimus* (also used in previous orientation studies), these spiders are common inhabitants of herbaceous old fields, they readily navigate through vegetation (Hill 1977a) and they perform well in a laboratory setting (Hill 1978, 2006a, 2010).

Spiders were photographed during jumps with the apparatus shown in Figure 2. The estimation of take off position was critical to measurement of take off velocity.

Figure 2. Apparatus used to capture strobe light photographs of spiders in flight. In each case the spider was placed in a starting position on a structure situated at the plane of focus. The strobe light was turned on, and the spider was stimulated into action with a dead fly (lure) attached to a long hair. In some cases, a jump directly toward the lure (prey) was elicited, and in other cases the lure was used to lead the spider to jump to a position closer to the lure, after the spider turned away from the lure. Each time that the spider prepared to jump, as indicated by the position of legs IV, the camera shutter was opened and then quickly closed to capture a series of pictures of the spider in flight. Photographs that did not record the starting position of the spider were not used. To avoid excessive light contamination, it was critical to open the shutter as close to the start of each jump as possible, and to immediately close the shutter at the conclusion of each flight.



As shown in Figures 3 and 4, slightly different methods were used to evaluate lateral versus dorsal photographs of spiders in flight. For lateral photographs (Figure 3), the contact point of leg IV with the substratum was used as a reference position (origin A or 0, 0) for the other measurements). Relative to this position, two successive positions in flight (C and D), separated by 15 msec, were measured from each photograph. These measurements were made as close to the launch or starting position of the spider as possible. For dorsal photographs (Figure 4), the center of a triangle connecting posterior lateral eyes (PLE) with the pedicel of the spider was used as a reference position for measurements. Otherwise, the approach to these measurements was the same. Only jumps for which these reference positions could be clearly measured (i.e., the starting position of the spider appeared in the photograph) were used in the calculation of take-off velocity.

Figure 3. Method used for estimation of take off position and computation of take off velocity for lateral views. A reference position near the center of gravity was plotted as the center of a triangle connecting the pedicel with the coxa of leg IV and the posterior lateral eye (PLE). Photographs were enlarged approximately 3 X and (x, y) coordinates of positions (A), (C), and (D) were measured. Based on measurements of adult female *Phidippus princeps*, as well as photographs with maximum leg extension, full extension of leg IV at the take off position was estimated to occur when the take off position (B) was 10 mm from the point of contact of leg IV with the surface (A). In most cases, position (B) was not photographed, and the closest positions (C) and (D) were used to calculate the flight trajectory, based on the 15 msec interval between plotted positions (C) and (D). The take off position (B), direction of take off velocity relative to a horizontal plane ( $\gamma_o$ ), and magnitude of take off velocity ( $V_o$ ) were computed as the intersection of the circle (A, B) and the flight trajectory through successive approximation.

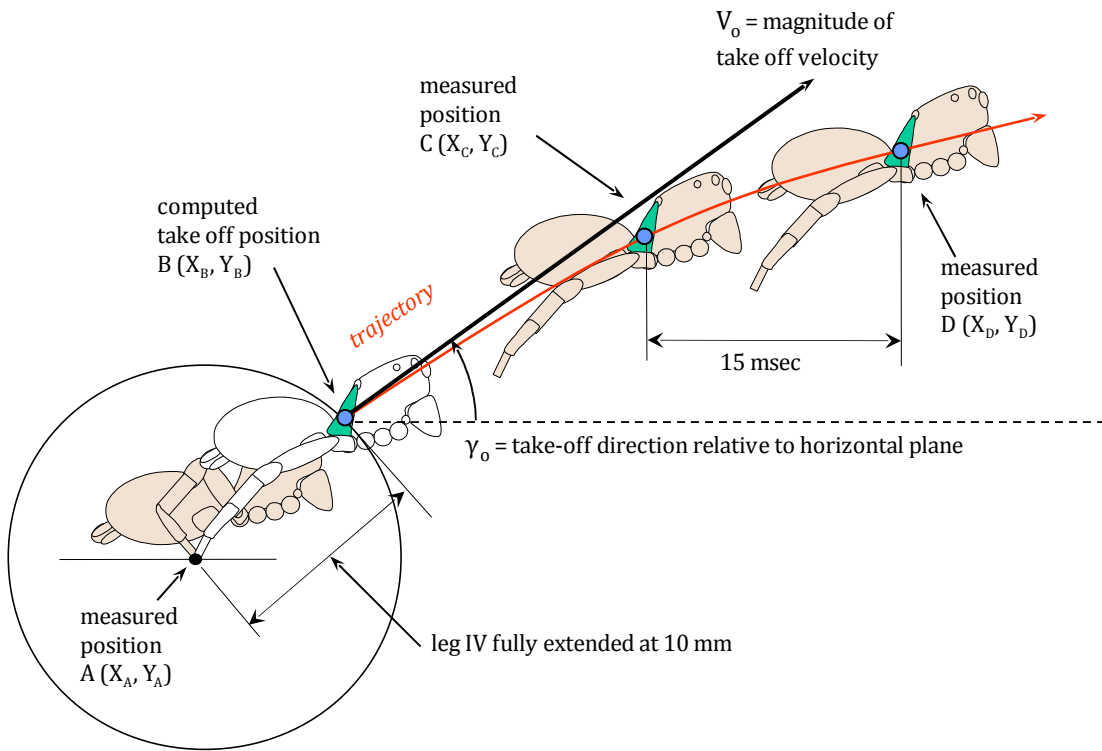
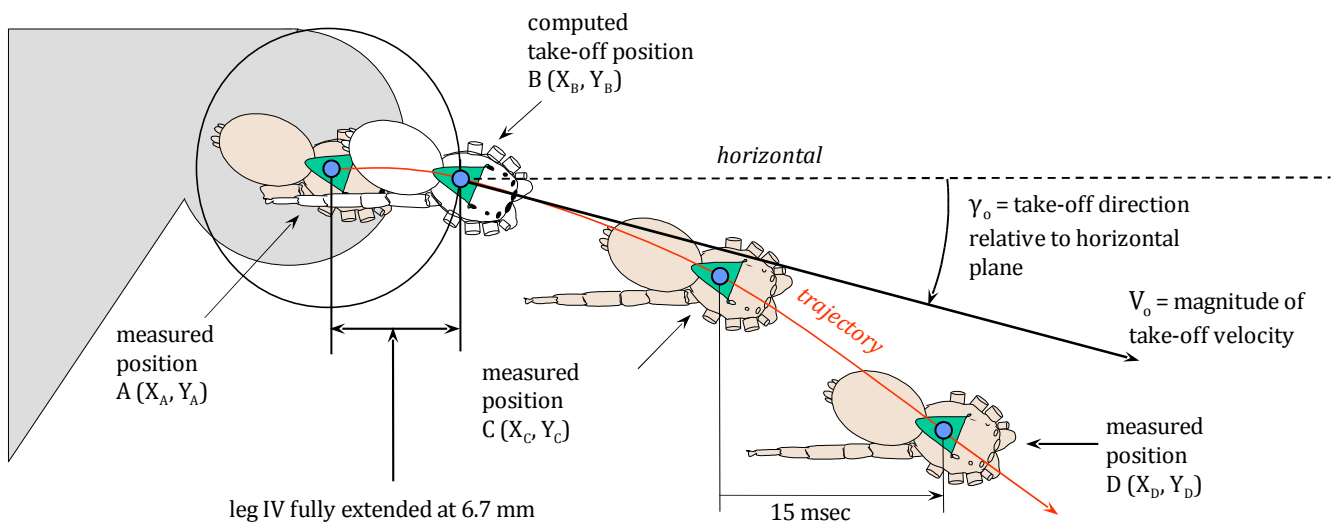


Figure 4. Method used for estimation of take off position and computation of take off velocity for dorsal views. Methods were similar to those used for lateral views (Figure 3), except that the center of gravity reference position was estimated as the center of a triangle connecting the pedicel to both posterior lateral eyes (PLE) of the spider. From measurements of spiders the take off position was determined to be near the position where this reference triangle had moved 6.7 mm from the starting position.



Measurements were made directly from negative projections with an enlarger, to maximize visibility of details in each picture. In one later study (Series 7), measurements were made with a pixel plotter on a computer screen. For future studies, this will be the preferred method for measurement of distances and angles. Measurements for positions (C) and (D) relative to (A) were taken from photographs and were then input into a computer program (Appendix 1) to calculate both the magnitude of take off velocity ( $V_o$ ), and the direction of take off velocity relative to a horizontal plane ( $\gamma_o$ ). The general method was to first compute the take off position ( $X_B, Y_B$ ), or intersection between the trajectory and the take-off reference circle, through successive approximation. This formed the basis for calculation of the take off velocity at position B, as follows:

*Define reference positions using X as horizontal distance and Y as vertical distance:*

$$[1] X_A = 0 \quad (cm)$$

$$[2] Y_A = 0 \quad (cm)$$

*Calculate the horizontal component of velocity ( $V_x$ ) during flight:*

$$[3] V_x = \frac{X_D - X_C}{T_1} \quad (cm/sec)$$

*(where  $T_1$  was the inter-flash interval of 0.015 sec)*

*Calculate the vertical component of velocity at position C ( $V_{YC}$ ):*

$$[4] V_{YC} = \frac{Y_D - Y_C}{T_1} - \frac{1}{2} g T_1^2 \quad (cm/sec)$$

*(where  $g$  was acceleration due to gravity,  $-980.7 \text{ cm/sec}^2$ )*

*Estimate the starting horizontal position ( $X_B$ ) as a value less than  $X_C$ :*

$$[5] X_B = X_C - 0.1 \quad (cm)$$

*Calculate the time interval between positions B and C ( $T_{BC}$ ):*

$$[6] T_{BC} = \frac{X_C - X_B}{V_x} \quad (sec)$$

*Calculate the vertical starting position ( $Y_B$ ):*

$$[7] Y_B = Y_C - V_{YC} T_{BC} + \frac{1}{2} g T_{BC}^2 \quad (cm)$$

*Calculate the radius of the take off circle, R:*

$$[8] R = \sqrt{X_B^2 + Y_B^2} \quad (cm)$$

Steps [5]–[8] were repeated, with step-wise *decrements* of 0.1 cm in the estimate for  $X_B$  [5], until the calculated R was less than the actual radius of the take off circle. Then steps [5]–[8] were repeated with an increment of 0.01 cm until the calculated R was greater than the radius of the take off circle. This process of successive approximation, alternating decrements with increments at successively lower values, continued to the level of 0.0000001 cm. The final values for position B ( $X_B$  and  $Y_B$ ) and  $T_{BC}$  were taken from the last cycle of calculations. These values were then used to calculate the magnitude and

directional components of take off velocity at position B as follows:

Calculate the horizontal component of velocity at position B ( $V_{YB}$ ):

$$[9] V_{YB} = V_{YC} - gT_{BC} \quad (\text{cm/sec})$$

Calculate the magnitude of the take off velocity at position B ( $V_o$ ):

$$[10] V_o = \sqrt{V_X^2 + V_{YB}^2} \quad (\text{cm/sec})$$

Calculate the direction of the take off velocity relative to a horizontal plane ( $\gamma_o$ ):

$$[11] \gamma_o = \arctan \left( \frac{V_{YB}}{V_X} \right) \quad (\text{degrees})$$

Measurement of pitch during jumps (angular velocity  $\omega_P$  in degrees/msec) was based on measurement of the relative direction of the apparent long axis of each spider through the center of gravity. Roll (angular velocity  $\omega_R$ ) was not measured directly but was estimated by visual examination of sequential photographs, based on the apparent inclination of the optic quadrangle at the top of the carapace (as defined by the ALE and PLE). The specific spatial configuration of each series of jump trials will be described with the respective results.

For quick reference, a chart that relates maximum horizontal range to take off velocity is provided in Appendix 2.

## 4. Results

### *Jumps to a target position*

As shown in Figure 5, the first trials compared jumps to positions at a horizontal distance of either 3 cm (Series 1) or 6 cm (Series 2). Jumps at a horizontal distance of 6 cm (Series 2) were also compared to 6 cm jumps at an inclination ( $\gamma_T$ ) of either  $-30^\circ$  (Series 3) or  $-60^\circ$  (Series 4) relative to a horizontal reference plane. All of these trials (Series 1–4) were completed with a single female *Phidippus princeps*. The spider was induced to jump to the target position through the use of a lure that was so distant that it could not be attacked directly. Previously (Hill 1978, 1979, 2006a, 2010) I found that these spiders would actively pursue intermediate positions (or *secondary objectives*) that allowed them to indirectly attain objective positions or targets (*detoured pursuit*). In these trials, the target position was a secondary objective. As shown in Figure 6, horizontal jumps to a position at 6 cm were significantly faster and higher than were horizontal jumps to a position at 3 cm. Jumps to a position at 6 cm were also significantly slower and aimed more directly toward the prey as the inclination of the target direction increased.

Figure 5. Layout of jump apparatus for jumps between positions (Series 1–4). In each case, the spider was engaged with a lure, which led the spider to attempt a jump to an intermediate position that would allow the spider to continue its pursuit of the sighted prey.

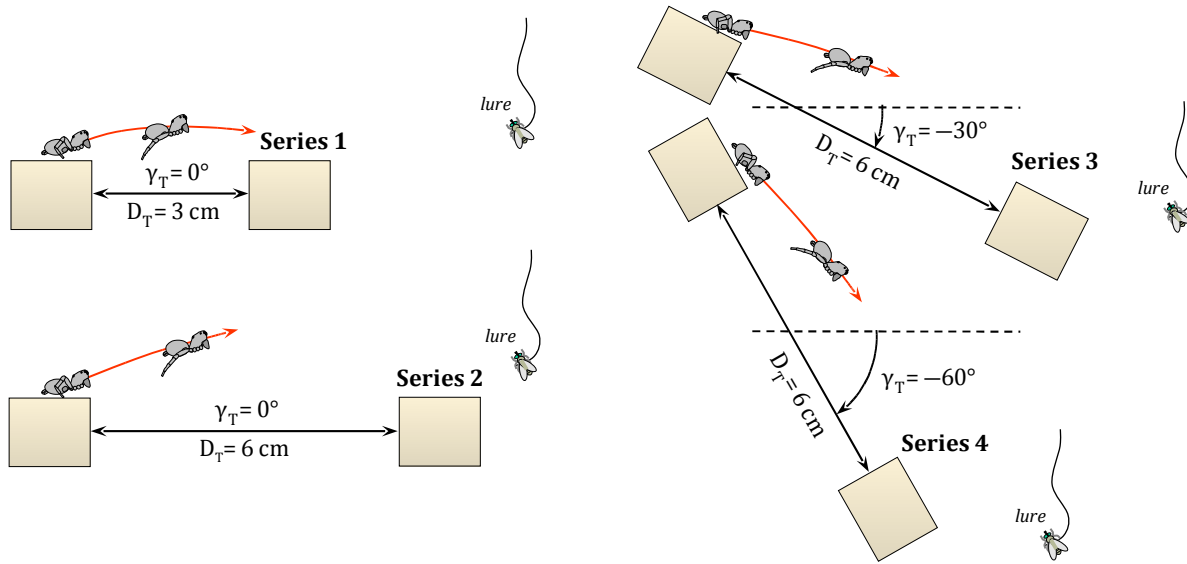
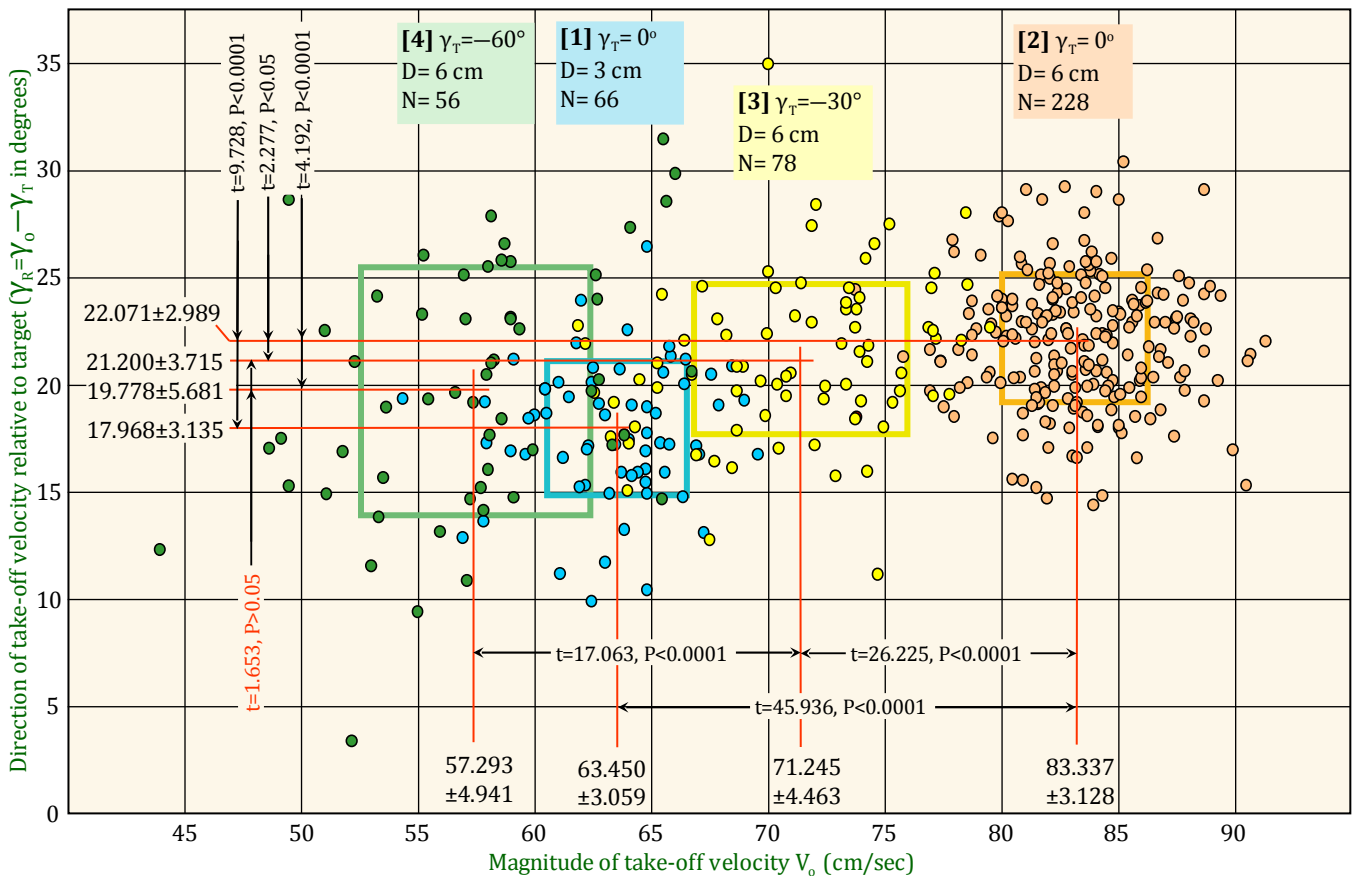
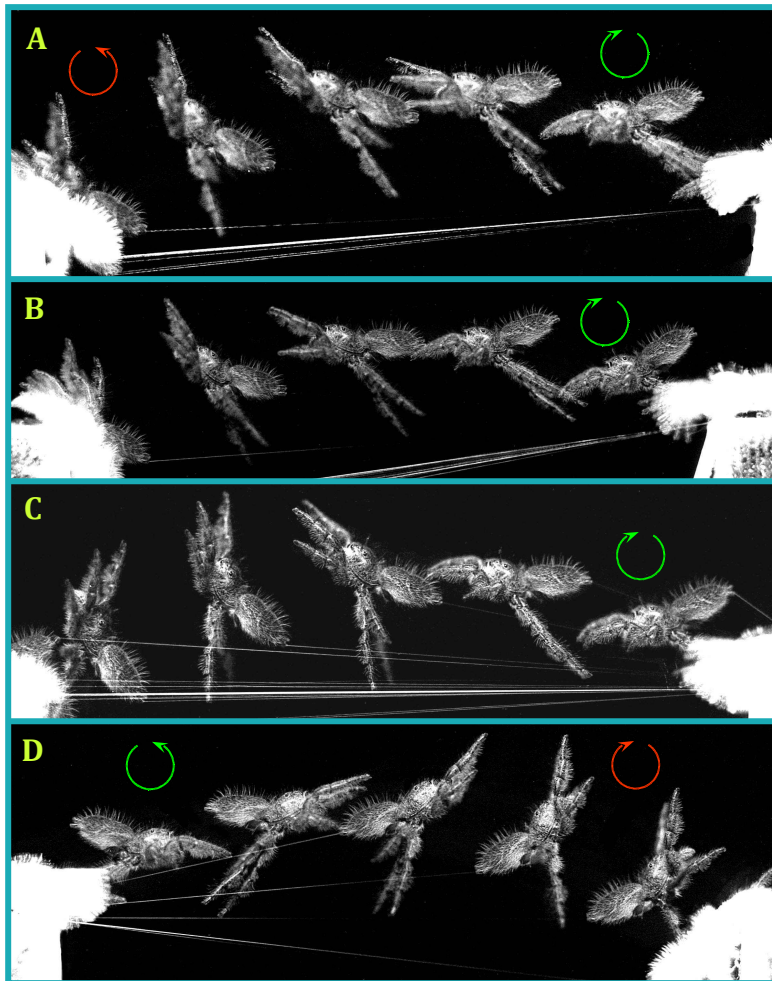


Figure 6 (below). Results of jump Series 1–4 (platform to platform). All measurements were based on jumps by a single adult female *Phidippus princeps*. Each point represents the magnitude ( $V_0$ ) and the direction of take-off velocity, expressed as the relative direction, or the difference between the measured take-off direction and the target direction ( $\gamma_0 - \gamma_T$ ). Distributions for each series ( $\pm 1$  standard deviation in either direction) are indicated in rectangles. Means (red lines intersecting at the mean position for each series) are depicted  $\pm 1$  standard deviation in each case, and arrows indicate statistical comparisons (one-tailed  $t$  test) for differences between mean values for respective distributions. Comparison of results for [1] to [2] shows that  $V_0$  was much greater for the 6 cm jump than for the 3 cm jump. Relative direction ( $\gamma_0 - \gamma_T$ ) was also significantly higher. Comparison of [2] with [3] and [4] shows that  $V_0$  increased, and the relative direction was higher, as the inclination of the target direction decreased.



Four examples of jumps from Series 2 are shown in Figure 7. Since these were horizontal jumps, they required a relatively high take-off velocity (average 83 cm/sec), but there was little apparent braking on the dragline (sudden change in velocity) associated with the relatively short distance of each jump. What can be seen clearly in these examples is the backward pitch that was characteristic of most jumps made by *Phidippus*. This essentially brought the spiders from a position where they faced the target position, to a position where the ventral side or sternum of the spider faced the target position.

Figure 7. Four 6 cm horizontal jumps by adult female *Phidippus princeps*, from Series 2. Successive photographs were separated by an interval of 15 msec. Note the forward extension of legs I and II, and the rearward extension of legs III and IV, during ballistic flight. The dragline was connected and taut in all cases. The backward pitch shown here (green arc) was characteristic of all jumps in Series 1–4. On shorter jumps like this the impact of braking (reversal of pitch, red arc) was not very great. These were all *position to position* jumps as the spider was moving to a location that would allow it to get closer to the sighted prey (the standard lure).



### *Jumps toward prey at a variable distance*

To evaluate the impact of prey distance on velocity, an apparatus was constructed with a reference hair extending from a platform down at an inclination of  $-60$  degrees relative to the horizontal (Figure 8, Series 5). The lure in each case was held at this constant direction but also at a variable distance. Lure distance ( $D_T$ ) was calculated relative to the starting reference position from measurements made directly from each photograph. For comparison with lure distance, the *range* of each measured trajectory in a

$-60^\circ$  direction ( $D_R$ ) was also computed as shown in Figure 6, as the distance of the intersection between the trajectory and a  $-60^\circ$  line drawn from the starting position. All Series 5 jumps shown in this study were associated with a single adult female *Phidippus princeps*.

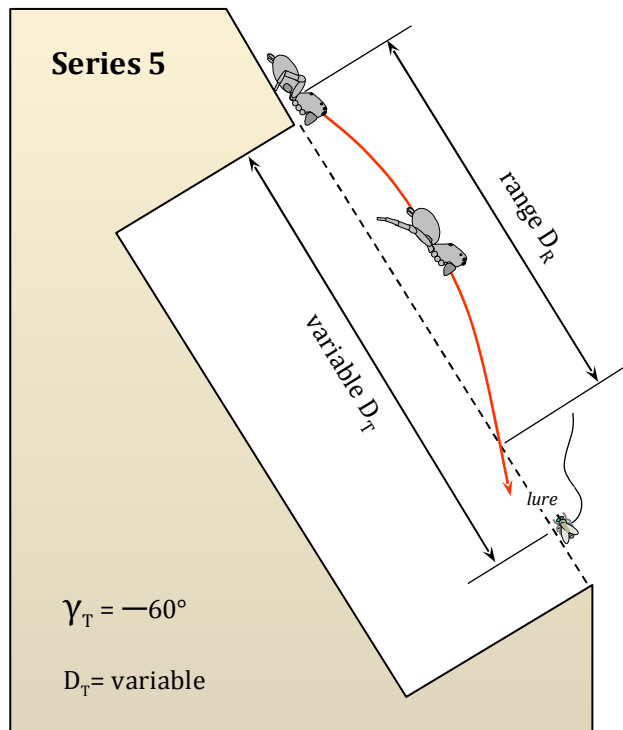
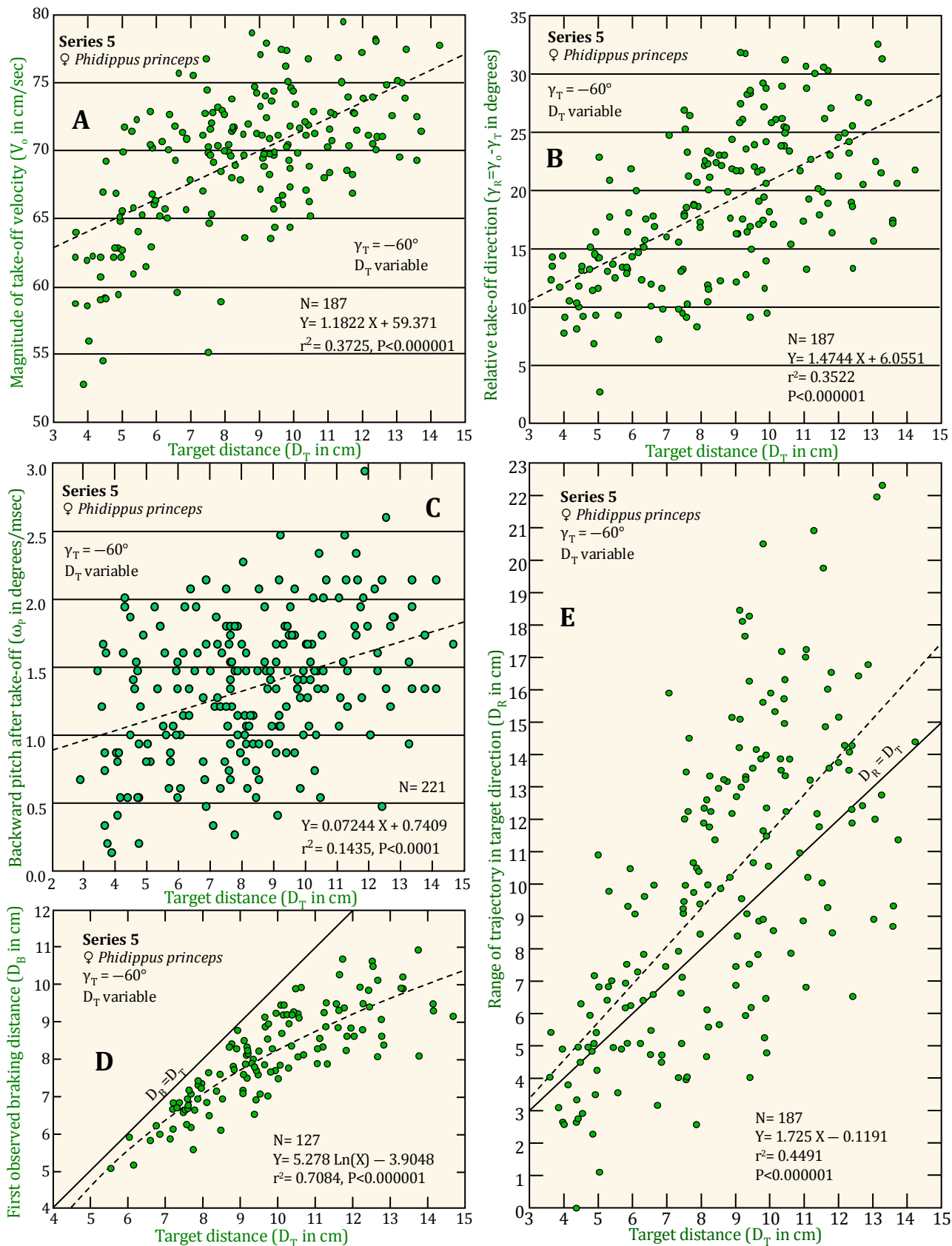


Figure 8. Jump apparatus for jumps toward prey at a variable distance, at a fixed direction ( $-60^\circ$ ) relative to the horizontal plane (Series 5). In this case, the lure was present at the time of each jump. Range was also computed as the distance of the intersection of the computed trajectory with the lure direction, for each jump.

With variable target distance ( $D_T$ ) at a constant target direction ( $\gamma_T$ ) of  $-60$  degrees relative to the horizontal both the magnitude of the take-off velocity ( $V_0$ ) and take-off direction relative to target direction ( $\gamma_0 - \gamma_T$ ) increased significantly as target distance increased (Figure 9). This spider jumped higher (relative to target direction) and faster to attain a greater range when the target was at a greater distance. Backward pitch was highly variable, but tended to be greater when the spider jumped at a higher velocity, toward a more distant target (Figure 9C). Jumps were not continuously filmed, but there was a significant correlation between the distance of the target and the distance at which braking on the dragline was clearly evident in the photographs taken at a 15 msec interval (Figure 9D).

Figure 9. Jumps toward prey presented to adult female *Phidippus princeps* at a variable distance ( $D_T$ ) in a constant direction ( $\gamma_T = -60^\circ$ ) (Series 5). A: The magnitude of take-off velocity ( $V_o$ ) was much greater for prey at a greater distance. B: Jumps at a greater distance were aimed ( $\gamma_o$ ) significantly higher at the onset, giving the spider a greater range. C: Backward pitch was seen in all jumps, but was significantly greater for longer jumps. D: Since photography was not continuous, only the first observed braking distance could be recorded. This represents the position of the first photograph where the pitch was reversed, for longer jumps where this occurred. E: Calculated range ( $D_R$ ) combined the impact of both  $V_o$  and  $\gamma_o$ , and the correlation with  $D_T$  was greater.



Representative jumps from Series 5 are shown in Figure 10. Braking on the dragline could be observed at each point where the backward pitch of the spider stopped or reversed. The detailed views in Figure 11 show that flight was close to the true ballistic trajectory until the point at which this braking began.

Figure 10. Representative Series 5 jumps. Photographs in each sequence were separated by an interval of 15 msec. Note the presence of a reference hair inclined at  $-60^\circ$  outside of the plane of each jump. Image A shows a jump with a relatively low range ( $D_R$ ) that nonetheless hit its target. Early in each jump there was a significant backward pitch ( $\omega_P$ ) in the flight of these spiders. The first photograph at which this pitch was obviously reversed through braking on the dragline is indicated with an arrow, for each series. After braking began, the legs flew forward in each case and came together in a catching basket (with the appearance of a terrestrial octopus!).

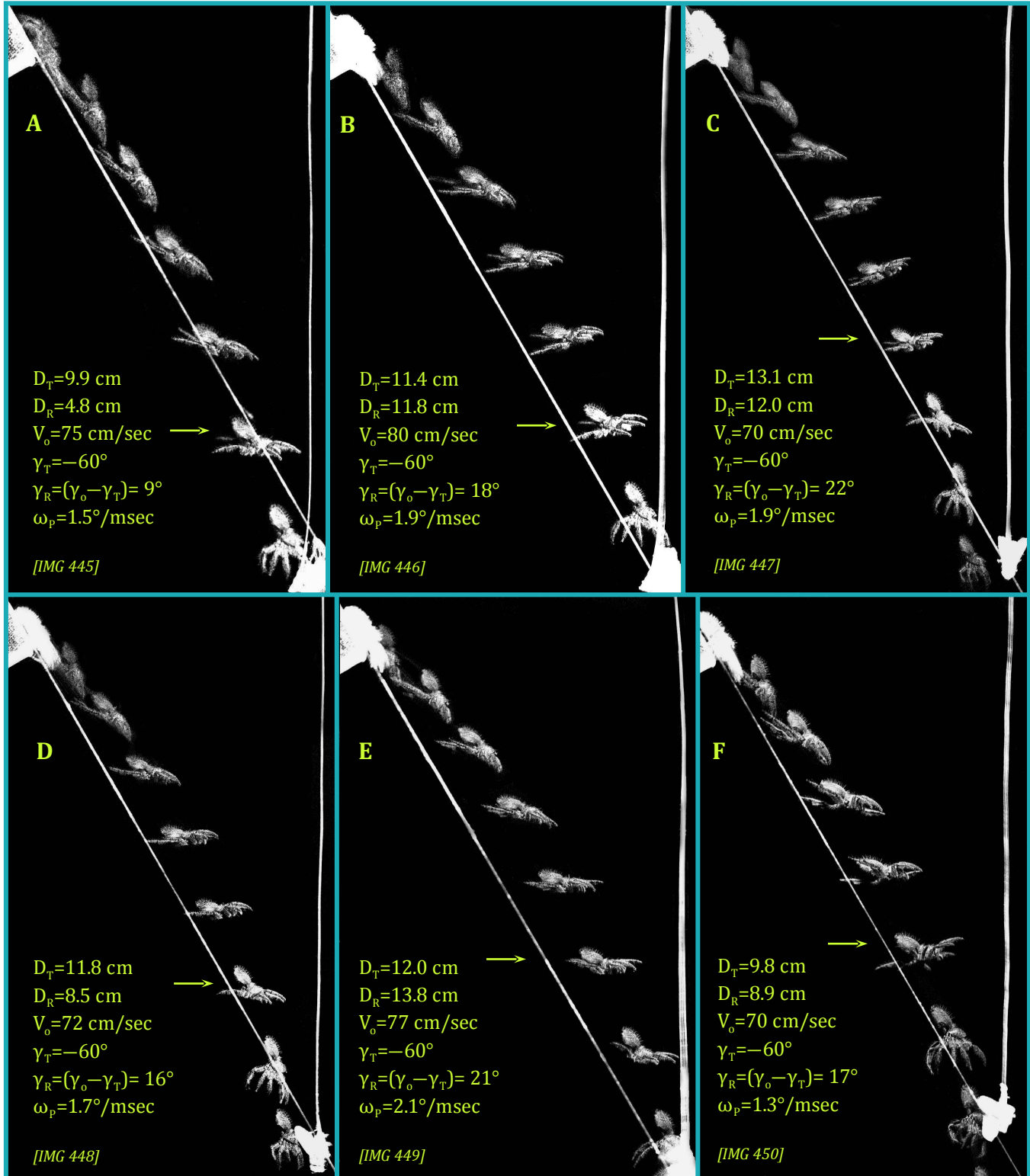
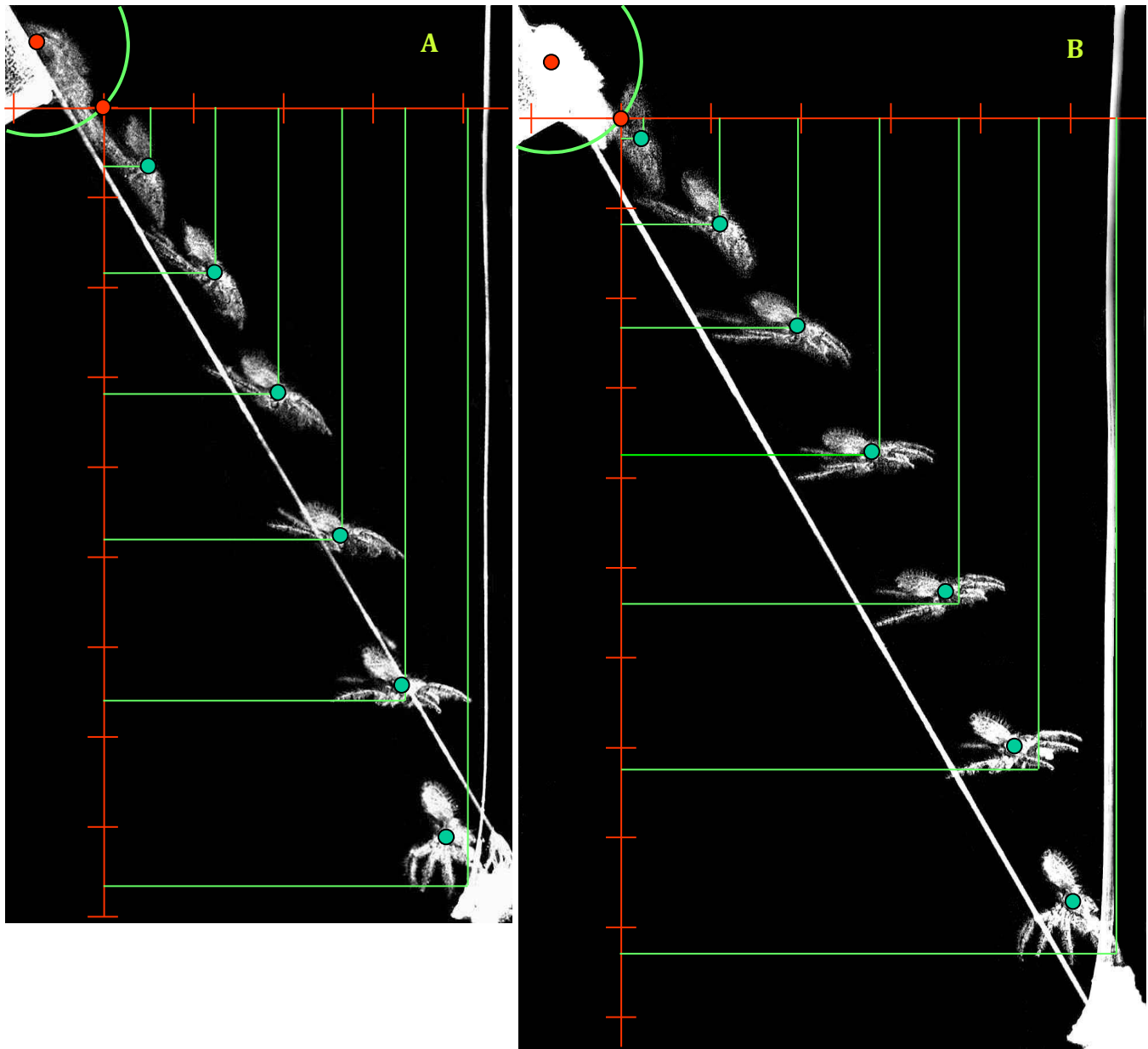


Figure 11. Detail of jumps A and B shown in Figure 10. X and Y axes (red lines), beginning at the calculated launch position, depict intervals of 1.00 cm. Successive positions of the center of gravity of the spider are plotted with green circles. The starting position of leg IV and the calculated take-off radius (large circle at upper left) are also shown. Horizontal and vertical lines depict calculated spider positions based on the calculated take off velocity and direction of take off, as if the flight took place in a vacuum. As can be seen, flights were essentially ballistic (free-fall) up to the point where dragline braking (associated with forward acceleration and stopping or reversal of backward pitch) could be seen with commensurate deviation from the ballistic path. Analyses like this also suggested that braking at the end of a flight could be completed in as little as 45 msec (or less), but it was not a factor in the early part of the flight. As can be seen from these examples, no evidence of gliding or significant air resistance was observed in the flight patterns of *Phidippus*.



*Jumps toward prey at a variable direction with respect to gravity*

To evaluate the impact of target direction relative to gravity on take off velocity, an apparatus was constructed that allowed the prey (lure) to be presented to the spider at a constant distance ( $D_T = 6$  cm), but at a variable direction ( $\gamma_T$ ) (Figure 12, Series 6). A dorsal view of positions was measured for each jump as shown in Figure 4. All Series 6 jumps shown in this study were associated with a single adult female *Phidippus princeps*.

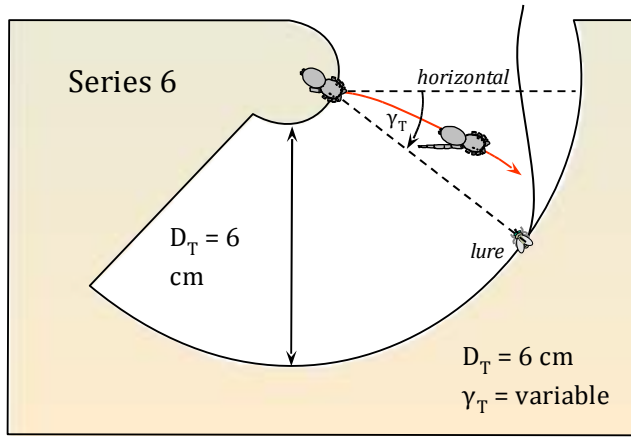
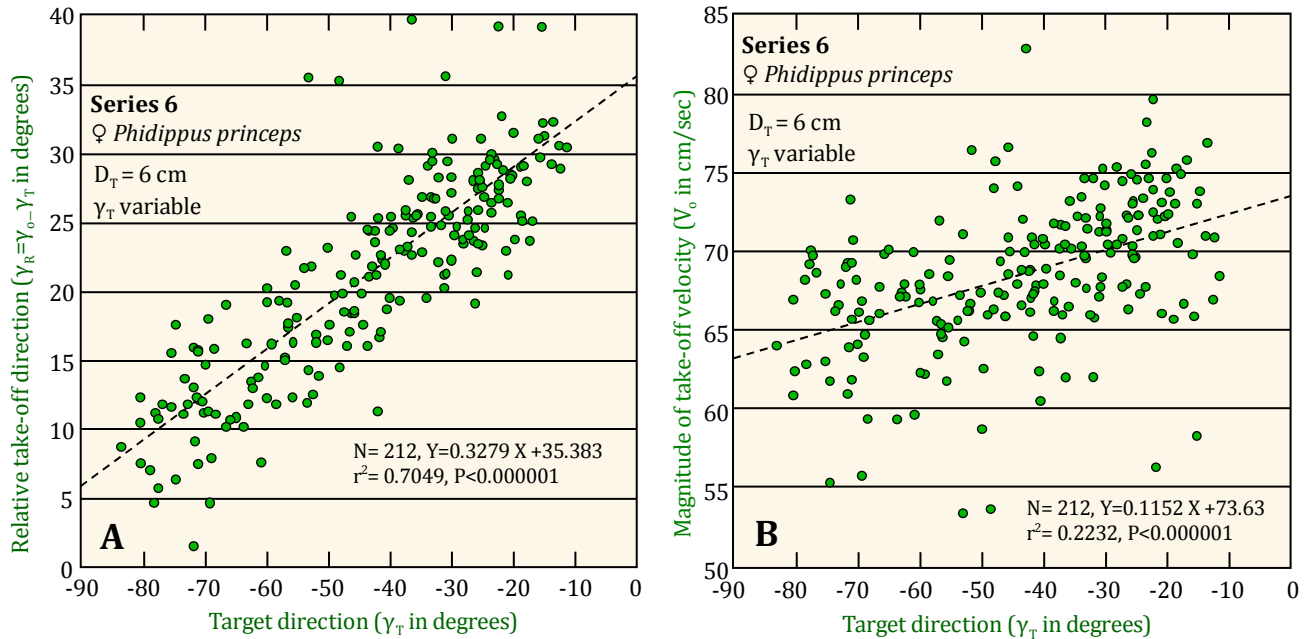


Figure 12. Jump apparatus for jumps toward a lure at a fixed distance (6 cm), at a variable direction relative to the horizontal plane ( $\gamma_T$ ). The lure was present at the time of each jump. For Series 6,  $D_T$  was 6 cm as shown here. For Series 7 jumps, a slightly different structure with  $D_T = 8$  cm was used.

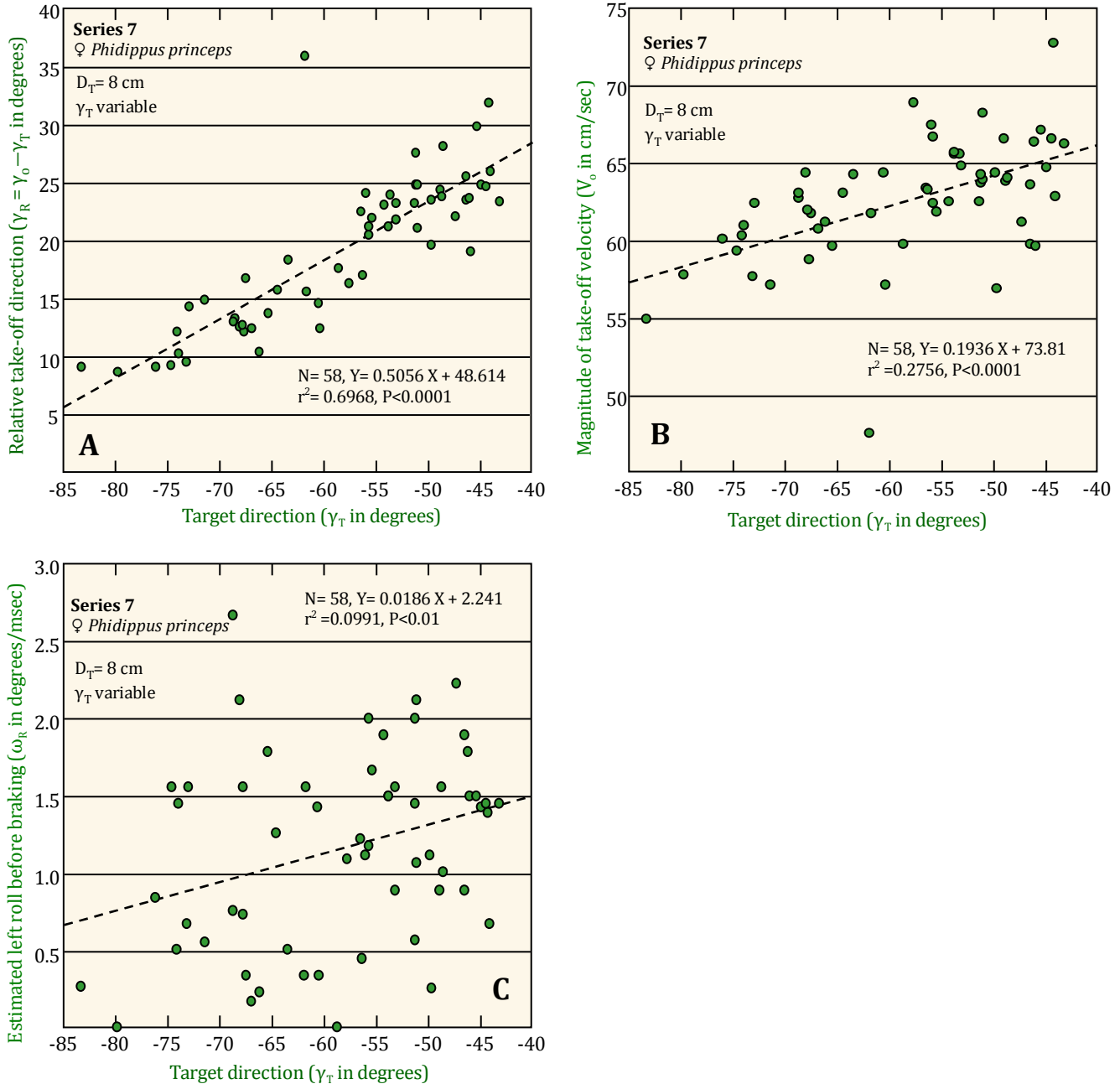
For jumps toward prey at a constant distance ( $D_T = 6$  cm; Series 6), this spider jumped progressively more directly toward the target (Figure 13A) and jumped more slowly (Figure 13B) as the target was positioned more directly under the spider (as  $\gamma_T$  approached  $-90^\circ$ ).

Figure 13. Jumps by adult female *Phidippus princeps* toward prey at a fixed distance and variable direction relative to gravity. Series 6 jumps were directed at a target at  $D_T = 6$  cm. A: Note the tight relationship between the relative direction of these jumps ( $\gamma_R = \gamma_0 - \gamma_T$ ) and the direction of the target with respect to gravity ( $\gamma_T$ ). B: Although there was more variability in the magnitude of take-off velocities, there was still a very significant tendency to make a faster jump when the direction of the target was closer to the horizontal ( $\gamma_T = 0^\circ$ ).



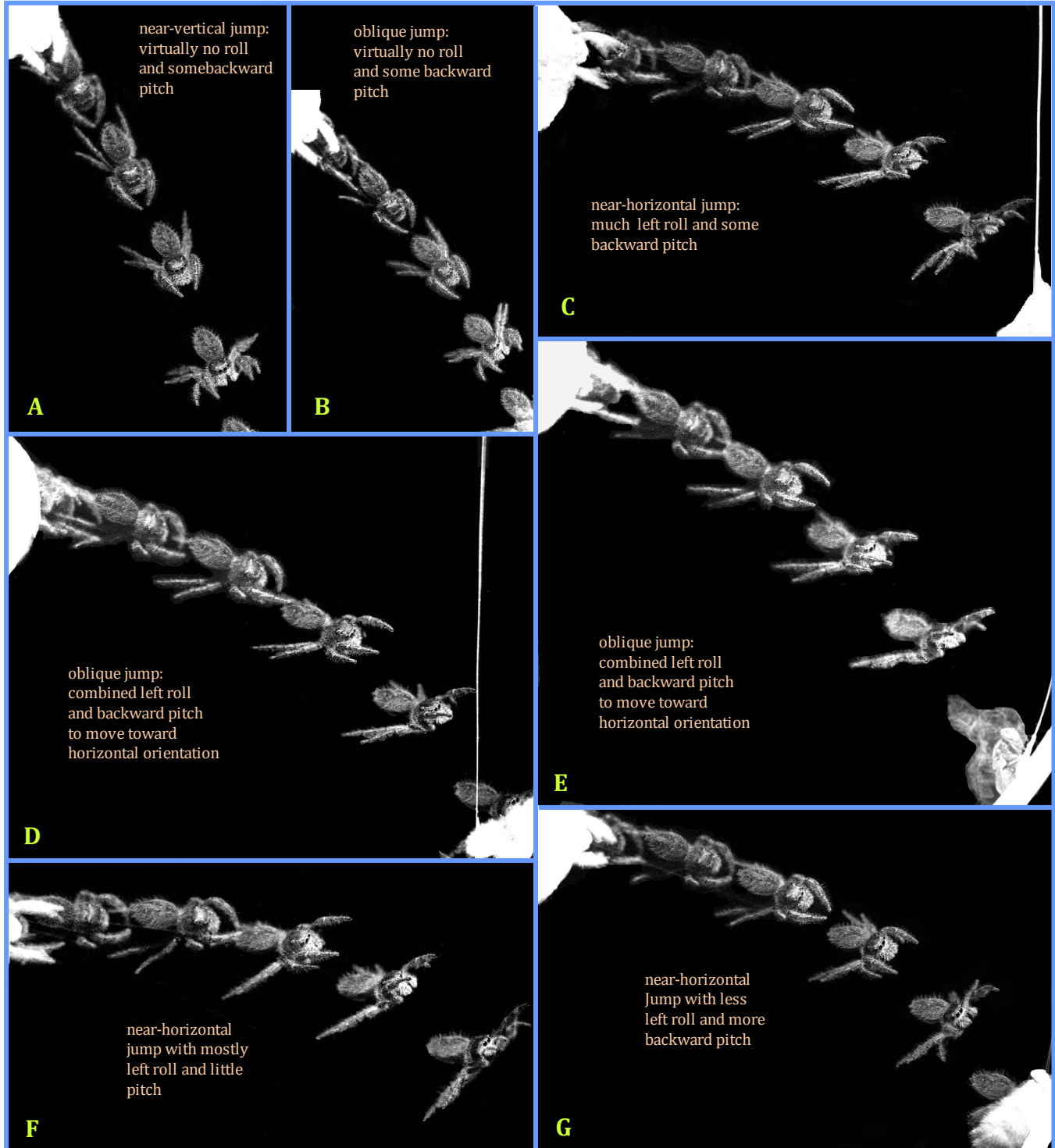
A second series (Series 7) of predatory jumps at a variable direction with respect to gravity, but at greater distance ( $D_T = 8$  cm) was recorded with a different female *P. princeps* (Figure 14). Over a more restricted range of target directions, the same strong correlation was observed between both the magnitude of take-off velocity ( $V_0$ ) and the take-off direction relative to the prey direction ( $\gamma_0 - \gamma_T$ ) with the direction of the target relative to gravity ( $\gamma_T$ ). These jumps (to the right) frequently included a component of *left roll* (counter-clockwise when viewed from the front of the spider, angular velocity  $\omega_R$ ) in addition to the normal backward pitch (angular velocity  $\omega_P$ ). For Series 7, the magnitude of this roll was estimated through visual examination of successive frames (Figure 14C). The roll tended to be less, or even non-existent, as the target was positioned more directly under the spider (as  $\gamma_T$  approached  $-90^\circ$ ).

Figure 14. Jumps by adult female *Phidippus princeps* toward prey at a fixed distance and variable direction relative to gravity. Series 7 jumps (different spider from that observed in Series 6) were directed at a more distant target  $D_T=8$  cm), and also covered a more limited range of directions. A and B: See Series 6 (Figure 13). C: This apparatus required a jump from a vertical plane. Jumps often included a component of roll ( $\omega_R$ ) in addition to pitch ( $\omega_P$ ) at take-off, as spiders rotated into a more horizontal position during flight (see also Figures 15 and 16). This roll was significant. This chart depicts estimated roll based on visual examination of the photographs, which did not allow for direct measurement. As shown here, roll was highly variable, but consistently to the *left* (per configuration shown in Figure 12), in a righting direction. Usually there was no roll when spiders jumped to prey that were directly below them ( $\gamma_T$  near  $-90^\circ$ ), and in these cases pitch alone would bring spiders closer to a horizontal orientation during flight.



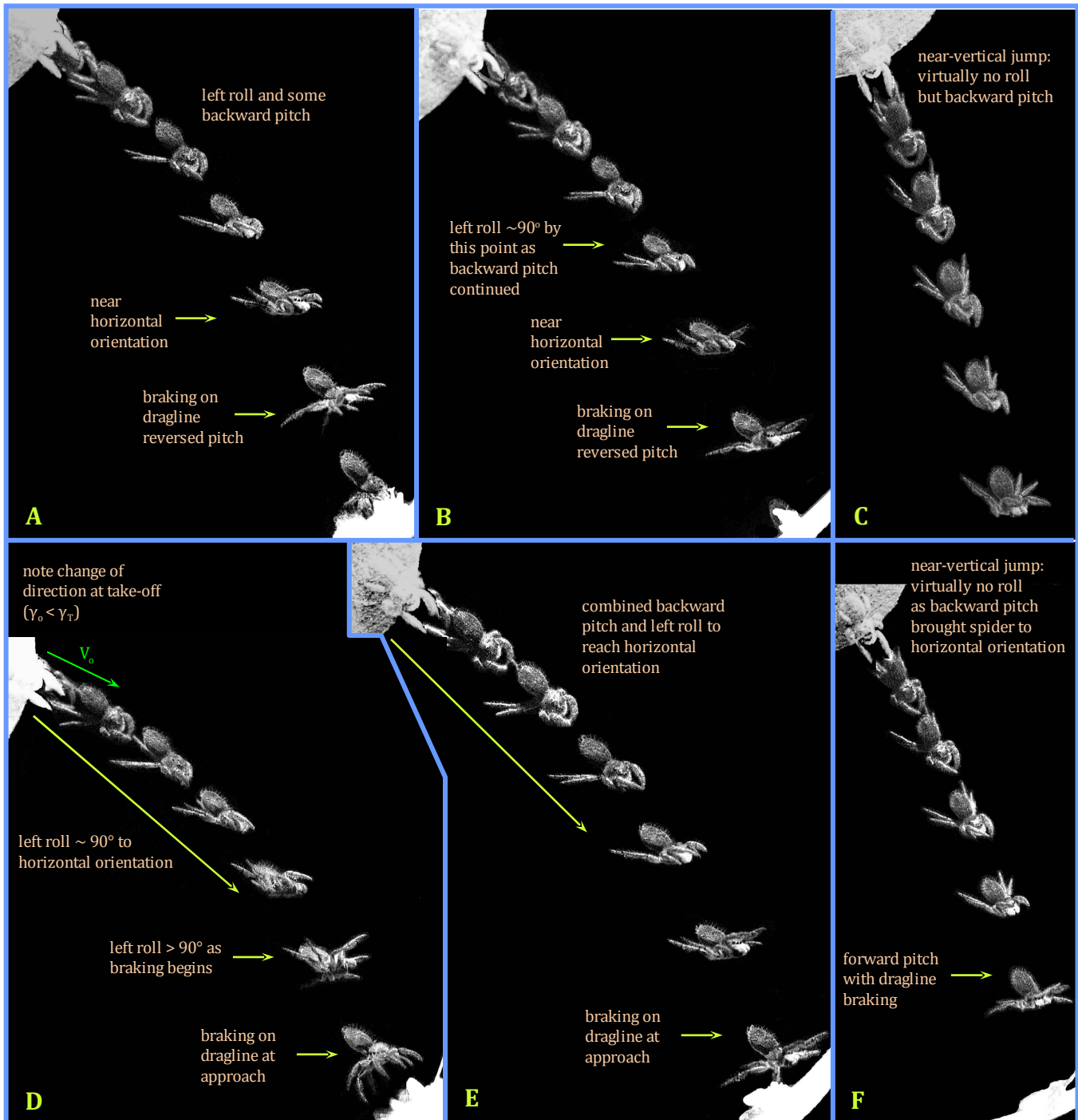
Representative jumps from Series 6 are shown in Figure 15. These illustrate clearly the combination of left roll and back pitch that brought this spider closer to a horizontal (right side up, dorsum at the top) orientation above the target during flight. As can be seen in Figure 15A–B, pitch contributed more to movement toward this orientation on near-vertical jumps.

Figure 15. Jumps by an adult female *Phidippus princeps* toward targets at a constant 6 cm distance, at a direction of  $-60^\circ$  relative to a horizontal plane (Series 6). A–B: Vertical or near-vertical jumps from a vertical surface were associated primarily with backward pitch, and little roll. This brought the spider toward a horizontal orientation (plane of horizontal section of prosoma horizontal with respect to gravity) as it approached the target. C–E: Left roll and backward pitch were both seen in most oblique jumps from this position, also bringing the spider closer to a horizontal orientation. F–G: The balance between left roll and backward pitch varied between jumps. As with most 6 cm jumps that were observed, dragline braking during flight was not as significant as it was on longer jumps. This may be related to the need for more dragline guidance (righting) on longer jumps.



For the longer jumps from Series 7 (Figure 16), dragline braking and reversal of pitch toward the end of each jump were more important. This observation was consistent with Series 5 results, which also showed that braking and reversal of pitch took place toward the end of longer jumps.

Figure 16. Jumps by an adult female *Phidippus princeps* toward targets at a longer (constant 8 cm) distance, at a direction of  $-60^\circ$  relative to a horizontal plane (Series 7). As on other longer jumps ( $> 6$  cm), braking on the dragline, as first indicated by the reversal of pitch by the telson (opisthosoma) was a consistent feature of these jumps. A–B: A near-horizontal orientation was achieved in most of these longer flights. C, F: Vertical or near-vertical jumps involved little roll, as backward pitch brought the spider closer to a horizontal orientation. D–E: Cumulative left roll, before braking, was close to  $90^\circ$  on many of these jumps. The rapidly rolling spider in (D) (near  $2^\circ$  left roll per msec) moved past the horizontal orientation before braking. Braking always had the effect of bringing the catching basket of the spider closer (sternum at center surrounded by spiny legs) to an orientation perpendicular to the net movement of the spider during its trajectory, as tracked by the dragline. On longer jumps, the dragline thus played a key role in flight control.



Comparison of jumps to prey with jumps to position

Two series were run where the spider (also an adult female *P. princeps*) was alternately given either a position (Series 8) or prey (Series 9) to jump at, on the same apparatus (similar to that used for Series 4, as shown in Figure 5), and at the same distance ( $D_T = 6$  cm) and direction relative to gravity ( $\gamma_T = -60^\circ$ ). Results (Figure 17) show that this spider jumped much faster toward the prey than toward the position. Because the same platform was visible to the spider, at the same distance, in both series, it is likely that this result was not due to any difference in estimation of distance by the spider, but that it represented a real tendency to move more quickly toward prey.

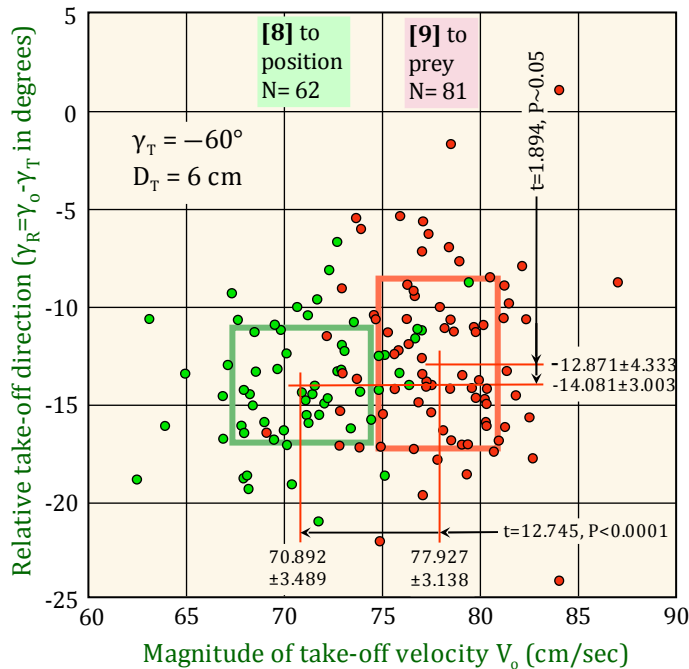
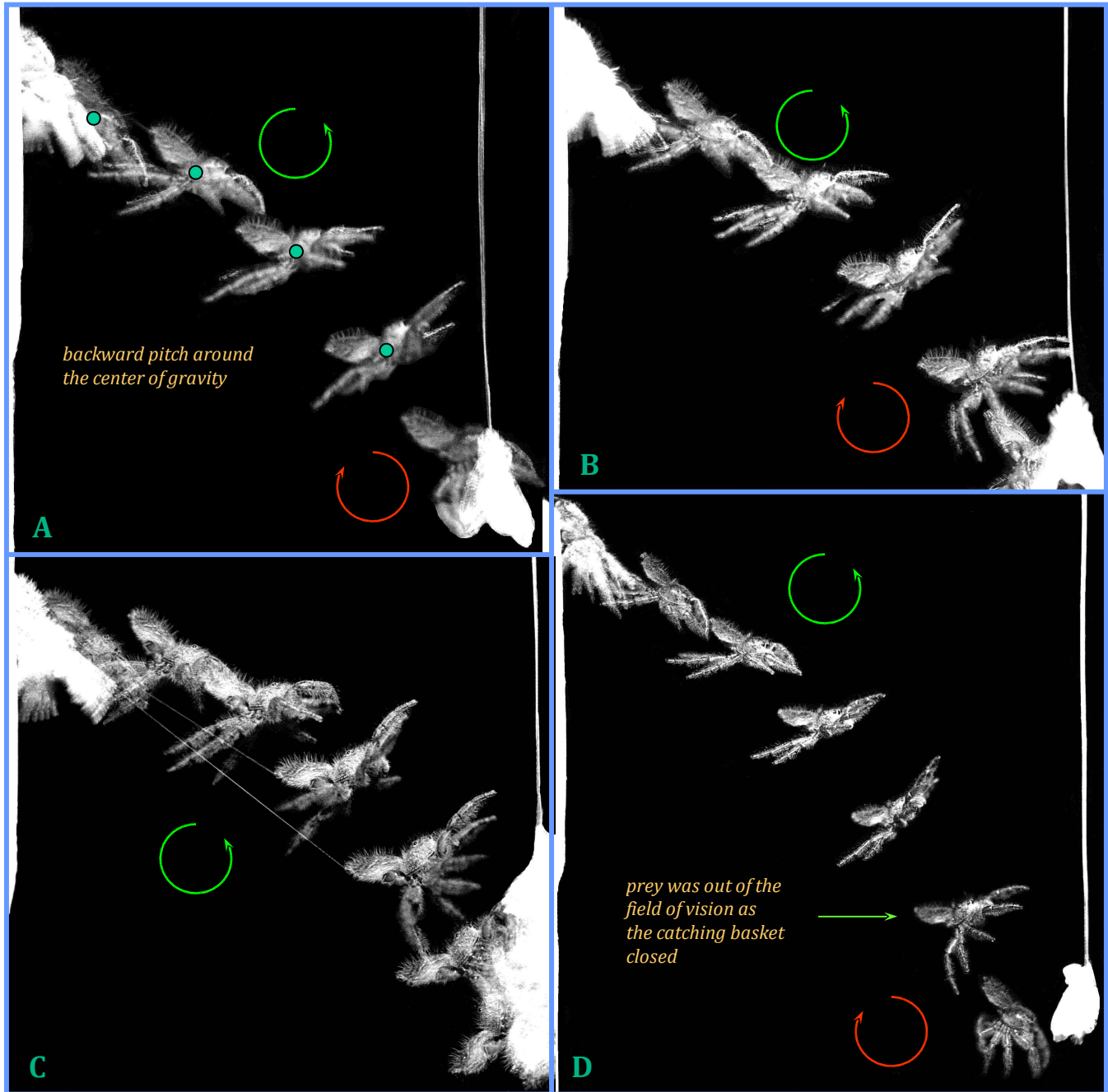


Figure 17. Jumps by an adult female *Phidippus princeps* toward targets at a constant 6 cm distance, at a direction of  $-60^\circ$  relative to a horizontal plane. The apparatus used for these jumps is shown in Figure 5 (Series 4). For Series 8, the spider jumped to an inclined platform (position), and for Series 9, the spider jumped to a lure (prey) at the same position as the edge of that platform. Boxes indicated  $\pm$  standard deviation from the mean for each set of trials. Mean values (intersecting red lines) are given  $\pm 1$  standard deviation. Significance of differences between respective means (arrows) were assessed with a one-tailed *t* test. This spider jumped significantly faster toward the prey at the same distance and direction relative to gravity.

Jumps off of a vertical surface

A vertical surface is constraining because, unlike a stem, it does not afford the spider the opportunity to execute a sideways jump. Examples of jumps by an adult female *P. princeps* off of a vertical surface are shown in Figure 18. Here the spider used *backward pitch* to approach the target in a horizontal orientation, above the target position. A back-flip of  $90^\circ$  was required. In all respects these jumps appeared to be just as accurate as jumps from other orientations. Even though a greater push off of the surface (perpendicular to the surface) was required to achieve this, jumps were also initiated well above the target direction in order to obtain the required range in ballistic flight.

Figure 18. Predatory jumps by an adult female *Phidippus princeps* off of a vertical surface. These jumps illustrate the importance of backward pitch to a salticid jumping down from a vertical structure. Spiders in this position readily execute a back-flip to catch prey with their legs facing in the opposite direction, away from the surface. During each approach during ballistic flight the target was out of the field of vision of the spider. A: Circles approximate the center of gravity of this spider to highlight its pitch ( $\omega_P$ ). D: On longer jumps such as this, braking and forward pitch near the prey position, toward the end of the jump, were more evident.

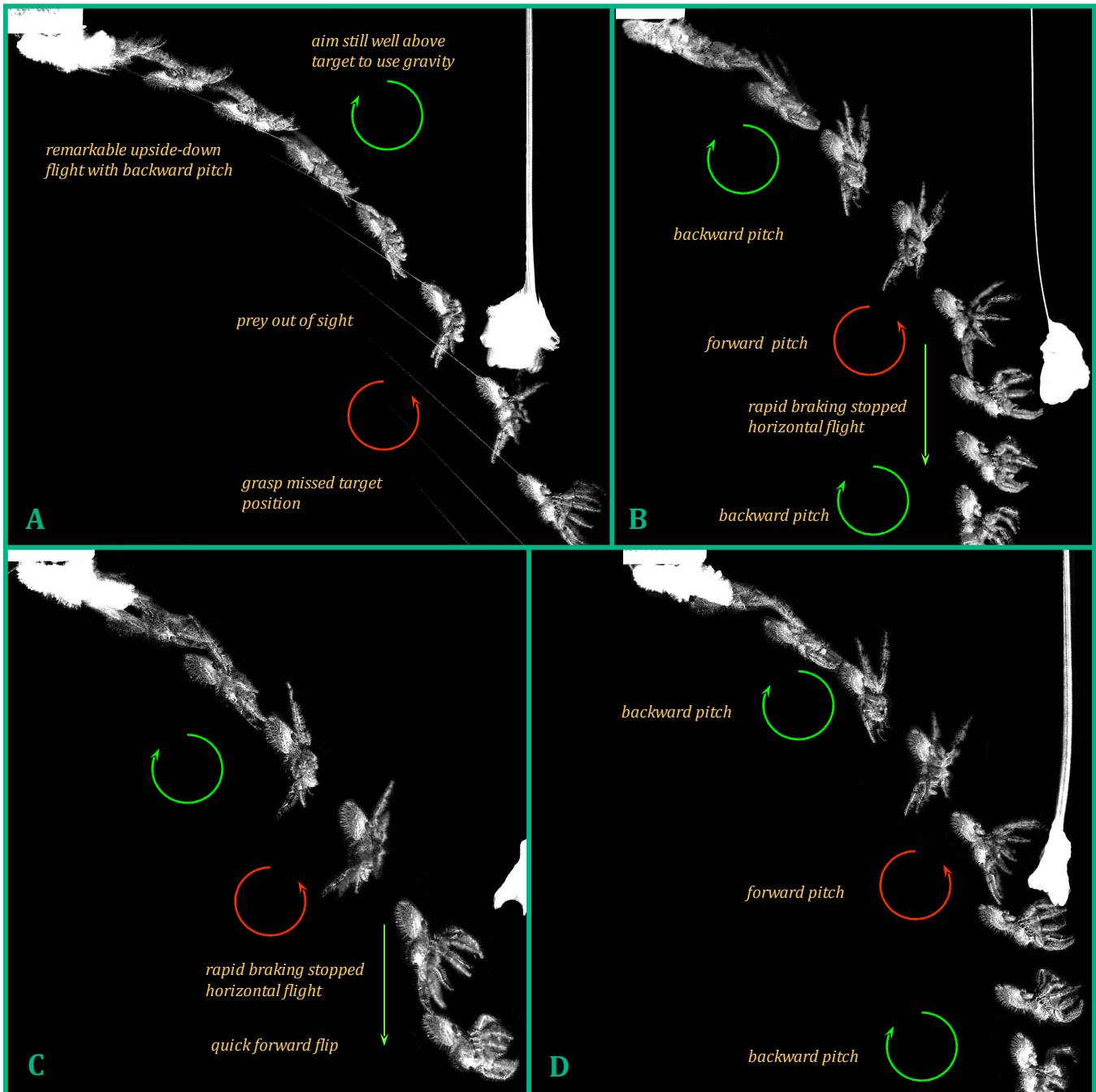


### Upside-down jumps beneath a horizontal surface

Jumps from an upside-down position would require the spider to complete a *roll* of  $180^\circ$  to obtain a horizontal orientation. Instead, spiders completed upside-down (dorsum of the spider facing down at the onset) jumps (Figure 19), using *backward pitch* to bring the legs into an orientation facing the prey. These jumps were remarkable in that the spiders still jumped well above the prey position in each case, *using gravity to fall upside-down* toward the target position during ballistic flight. In all respects jumps from this position appeared to be as accurate as those from other positions. Backward pitch was still a major

factor in these jumps, rotating the spider backward to orient the catching basket formed by the extended legs toward the target. Near the target braking also reversed the pitch, at least at first. One difference between a right-side up jump and an upside-down jump is that during pendulum movement, beyond the point of braking, pull and rotation of the spider—dragline pendulum reestablishes a backward pitch (or second reversal of pitch) when the spider is upside down (Figure 19B, D). During right-side up jumps, this pendulum action continues the forward pitch of the spider.

Figure 19. Upside-down predatory jumps by an adult female *Phidippus princeps* from beneath a horizontal surface. In upside-down flight the usual features of targeting above the prey position to gain range, backward pitch, and rapid braking followed by reversal of pitch near the prey position, were also seen. These jumps appeared to be just as accurate as right side-up (dorsum up) jumps from a horizontal surface. The rapid backward pitch at the bottom of B and D appeared to be the result of rapid recoil on the elastic dragline as forward pitch rotated the long axis of the spider past alignment with the dragline direction. Continued movement as a pendulum subject to the acceleration of gravity after braking creates forward pitch when the spider is right side-up, but it creates backward pitch when the spider is upside-down. Thus two successive reversals of pitch can be seen during an upside down flight.



## 5. Discussion

### *Spider measurement of direction and distance*

Earlier work established the ability of these spiders to measure the relative distance and direction of a target with respect to gravity. Memory of direction and position relative to gravity have been shown to be key factors in the ability of these spiders to retain a memory of relative prey position during the detoured pursuit of prey. These spiders have also been shown to retain a memory of the direction of prey relative to gravity after a missed jump (Hill 1978, 1979, 2006a, 2010). The demonstration that the take off velocity (both magnitude and direction) of salticids compensates for both distance and direction of a target relative to gravity represents one more demonstration of their ability to measure both distance and direction, at the same time that it illustrates one more aspect of the versatility of these spiders.

### *Use of gravity to increase range*

*Phidippus* readily move to positions from which they can utilize gravity to extend their range in order to attack distant prey. By moving prey toward these spiders from different directions, it has been easy to demonstrate that direction relative to gravity was a key determinant of the maximum distance at which a spider would launch an attack (Hill 1975, 1978, 2006a, 2010). Since flight is ballistic, direct jumps of any distance that did not compensate for the force of gravity would obviously miss their mark. Given the range of targeted jumps by *Phidippus* (10 cm or more), and the attainable magnitude of take off velocity (on the order of 80–90 cm/sec), the demonstrated ability to jump well above a position in order to fall down upon that position should not be surprising. As shown in the present study, these spiders used both variable speed and variable direction relative to prey or target position in order to achieve the required range for each jump. There is no reason to believe that this level of versatility is any less than that of a basketball player who evaluates target distance and direction and adjusts the velocity of the thrown basketball accordingly. The ability of *Phidippus* to use gravity to complete an accurate upside-down flight trajectory when jumping from an upside-down position (Figure 19) was remarkable by itself. Beyond this demonstration, salticids have been observed to jump from any plausible orientation to reach a target. For example, many readily jump from a rightside-up orientation on top of a leaf to an upside-down orientation on the underside of a higher leaf ( $\omega_P = 180^\circ$ ).

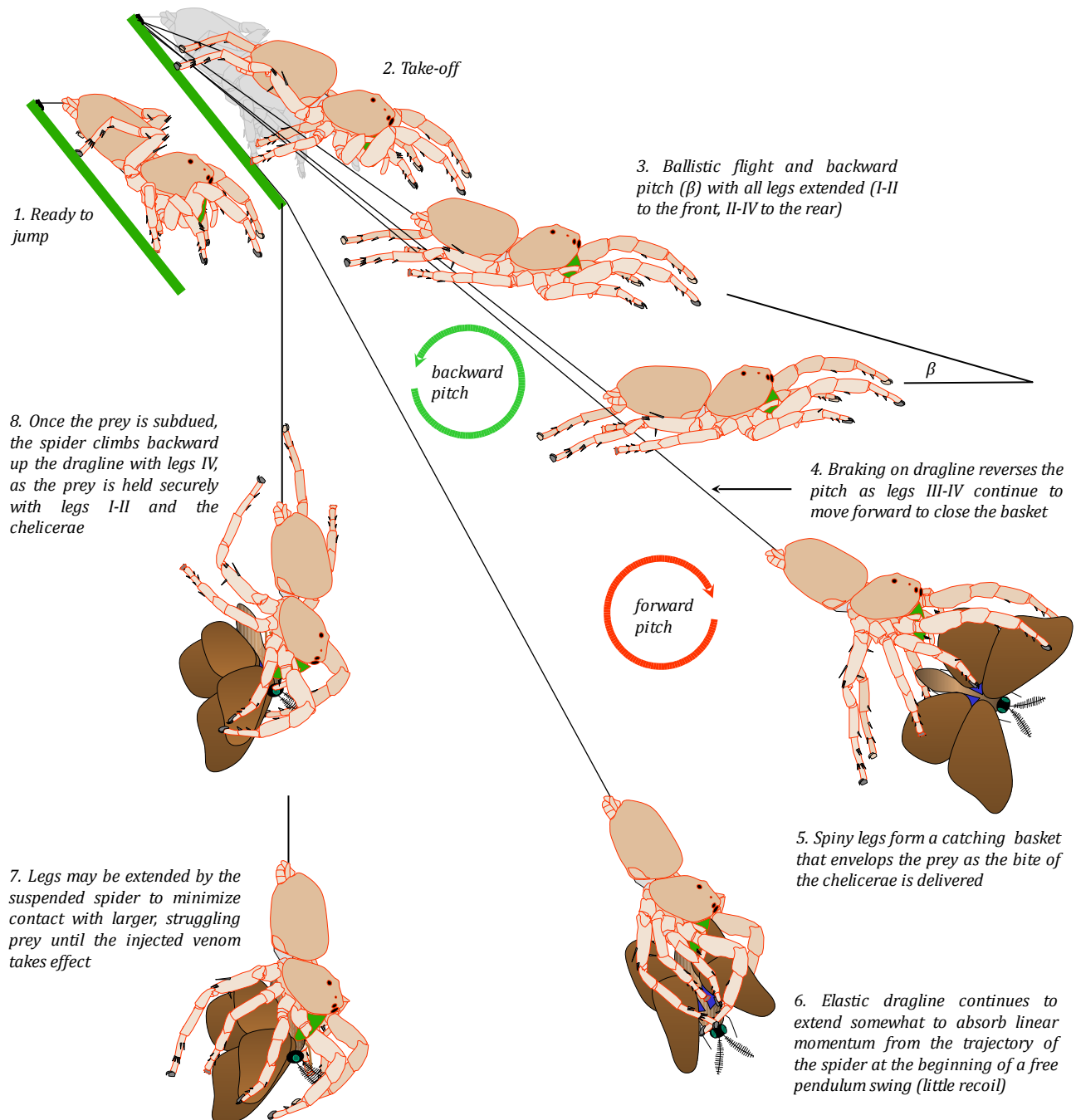
### *Ballistic flight*

The observed flight of *Phidippus* during jumps was essentially ballistic (see Figure 11) until they braked on the dragline. For the range and velocity of jumps shown here, air resistance (or gliding) effects were looked for, but were not observed. For smaller and lighter salticids, it is possible that some gliding effects could still be found. However, there are no obvious adaptations that would allow salticids to maintain control of their orientation during active gliding, free of the dragline. Euophryine Australian salticids of the genus *Maratus*, in which the males have conspicuous lateral flaps on the opisthosoma, were once thought to have the ability to glide (Pickard-Cambridge 1874). These flaps are now recognized as ornaments used in courtship (Waldock 2007, 2008, Hill 2009, Otto and Hill 2010).

### *General features of ranged predatory jumps*

Not all prey capture by *Phidippus* involves ranged jumps or long ballistic flights. When these spiders do jump toward prey, however, they can launch themselves on an accurate trajectory, and to orient the catching basket formed by their eight legs around the prey position during ballistic flight. General features of a ranged predatory jump are highlighted in Figure 20. Key elements of the predatory jump as shown here include the targeted ballistic trajectory, backward pitch during early flight, braking on the dragline during longer flight, and closing of the catching basket formed by all eight legs around the prey.

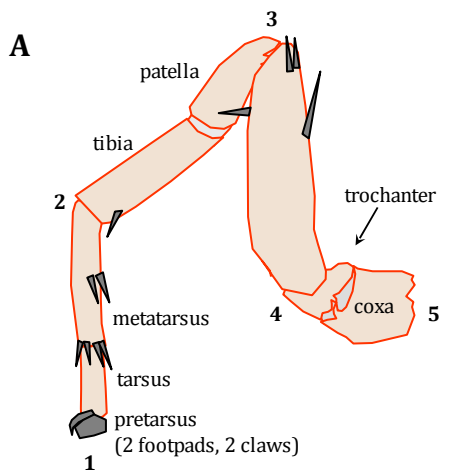
Figure 20. General features of ranged predatory jumps by *Phidippus* jumping spiders. This example does not include the roll and other flight dynamics that may be associated with jumps from positions where the symmetrical alignment of the jumping platform with the vertical plane of the jump does not exist, as shown here. After take-off, backward pitch ( $\omega_P$ ) brings spiders into a near-horizontal orientation (3), before dragline braking reverses this pitch (4) and the spiny legs of the spider move forward to grasp the prey (5). After prey is captured (6), the elastic dragline absorbs the linear momentum of the spider with little if any recoil, as the force of gravity continues to apply torque to the falling spider/dragline system, now a pendulum. As long as the hanging spider continues to fall as a pendulum, it continues to accelerate due to the force of gravity. The spider may remain suspended in a vertical position (7) for 5–15 seconds or longer, until the prey has been subdued. To ascend the dragline while holding prey, the spider usually climbs backward up the dragline as shown here (8), with alternating legs IV. I have also seen *Phidippus* rappel to a visible lower position by releasing additional dragline silk while suspended. If the prey was missed, the spider will catch the dragline with one leg IV, and will flip itself around to make a much faster forward ascent, winding up the dragline with legs I and II while holding legs III and IV outstretched. In this case the wound dragline is discarded near the original attachment disk. Note that the rotation of the legs to close the catching basket (5) is powered not only by the forward momentum of these legs, but it is also accelerated by torque associated with pull of the dragline on the body. Powerful flexor muscles of these spiders should play a key role in this rapid movement of the legs during prey capture.



## Biomechanics of the launch

On a flat horizontal surface, the take off posture of *Phidippus* suggests that the flexed legs IV normally provide most if not all of the propulsion for the jump. Legs I and II are typically extended and elevated, and legs III (and in some cases, legs II) provide a brace, fulcrum, or pivot point against the substratum. In other salticids such as *Habronattus* or even *Salticus* (Parry and Brown 1959b) it can be readily observed that legs III provide propulsion to the spider, so this specific mechanism is by no means universal in the Salticidae. I have not investigated this, but it is plausible that *Phidippus* could adapt to use legs III for propulsion if required to do so. Parry and Brown found that *Sitticus* jumping spiders also used legs IV to propel their jumps. They did not regard the role of legs III as significant, but they were considering only at the powering of jumps, and not the steering. A detailed assessment of the function of legs III and IV during the launch of *Phidippus* is presented here in Figures 21 and 22.

Figure 21. Movement of leg IV during take-off by *Phidippus* jumping spiders. This configuration applies to many other salticids (e.g., *Sitticus*, Parry and Brown 1959b), but not to all salticids. A: Reference diagram for articulation of segments and major joints related to extension of leg IV, which powers the jump. Extension at joints 2, 3, and 4 is most important, and some joints that allow limited flexibility in a lateral direction (e.g., the patello-tibial joint) are locked in the plane of leg extension during take-off. B: Diagrammatic view of launch system superimposed on photograph of adult female *Phidippus princeps*. Leg IV is highlighted in green. The large circle at center represents the center of gravity of the spider, and below it a smaller circle represents the articulation of leg IV with the body. Legs III, extending laterally and to the front, form a stable four-legged platform with legs IV during launch, and may be viewed as a fulcrum with respect to torque delivered by the extension of leg IV, at least during the onset of take-off. Legs II are also sometimes used for stabilization, but are usually held forward with legs I, off of the surface, during take-off. As shown here, an arc drawn through the center of gravity of the spider, with its center at the ground contact of legs III, approximates the direction faced by the spider at take off, and the initial direction of movement.



- 1 Footing (pretarsal setae/substratum)
- 2 Tibio-metatarsal joint
- 3 Femoro-patellar joint
- 4 Trochantro-femoral joint
- 5 Articulation with prosoma (coxa)

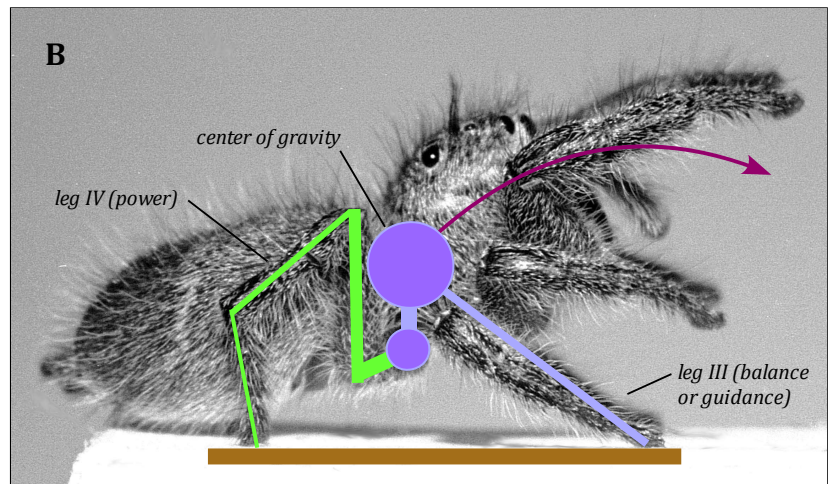
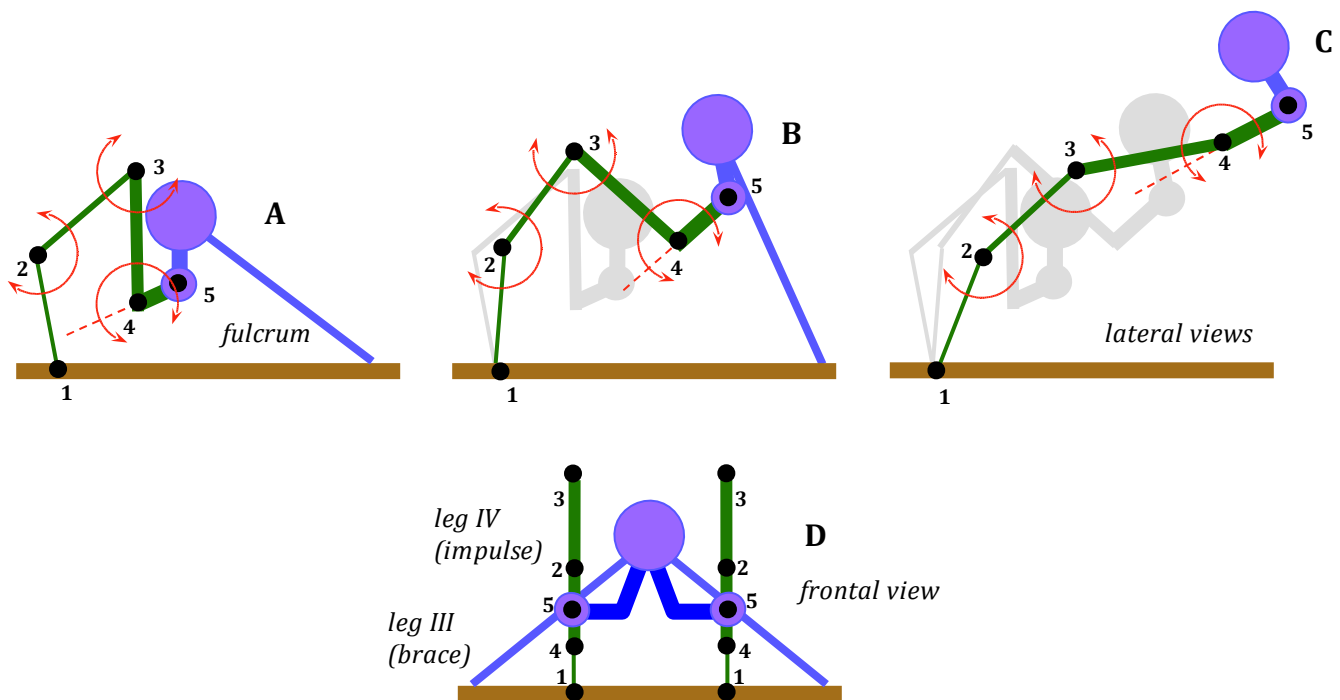


Figure 22. Movement of leg IV during take-off by *Phidippus* jumping spiders, based on leg segments identified in Figure 21. A–D: Model of joint and segment dynamics during launch. Particularly since the mass of the legs is relatively small compared to body mass, acceleration of leg segments is less important than is the ability of the extending legs to push down and backward against the substratum. As in all walking or jumping creatures, movement is caused by an equal and opposite ground reaction force. This is applied to the spider by the substratum in contact with the pretarsus of leg IV (position 1). Two-headed arcs (couples between segments, in red) represent the hydraulic expansion of joints 2, 3, and 4, respectively. Traction and resistance of the substratum to sudden leg extension is critical. Note the fact that the articulation of leg IV with the body occurs below the center of gravity. This separation can deliver a consistent torque around a transverse axis through the center of gravity, powering the back pitch ( $\omega_P$ ) that is normally observed as part of a salticid jump. Assymmetric application of force through left and right legs IV can account for the ability of these spiders to deliver roll ( $\omega_R$ ) at launch. Note the impact of the leverage applied by legs III on movement between positions A and B. This leverage, also involving application of force to the substratum with a commensurate ground reaction force of its own, appears to be important in controlling the direction of these jumps by constraining the direction of net movement of the center of gravity of the spider during launch. Obviously, without the platform support of legs III, the two-legged spider would fall over before it could jump! Consistent delivery of a yaw ( $\omega_Y$ , angular velocity about a vertical axis) impulse at launch has not been observed, but in theory could be delivered through asymmetric force or torque applied by legs on opposite sides of the body (as in the execution of an  $\rho$  facing turn by these spiders, Hill 2006a, 2010). The stable four-legged launch platform may serve as a brace to prevent yaw that could result from irregular delivery of force by legs IV during launch. This hypothesis is supported by the observation that legs III are frequently extended laterally prior to a jump (D), as if to brace against this kind of movement.



As shown in Figure 23, legs III and IV can be positioned in preparation for a jump to accommodate the requirements of movement in different directions relative to the orientation of the substratum. In a real-world situation, the relationship of the substratum to the trajectory can be much more complicated (Figure 24), and these spiders display much more versatility than can be readily demonstrated in a laboratory setting.

Figure 23. Relative alignment of legs III and IV to the body at the start of a jump in various directions from a horizontal surface (adult female *Phidippus princeps*). These alignments agree with those described previously for *Sitticus* (Parry and Brown 1959b). Note the relative position of the articulation of leg IV (small circle) with respect to the center of gravity (large circle) in each case, as well as significant differences in the placement of legs III. An arc through the center of gravity that is centered on the ground contact of leg III (purple arc) approximates the take-off direction, which is also the direction faced by the spider. Tarsal claws of legs IV face to the rear during take-off, and the paired foot pads of each leg are applied to the surface.

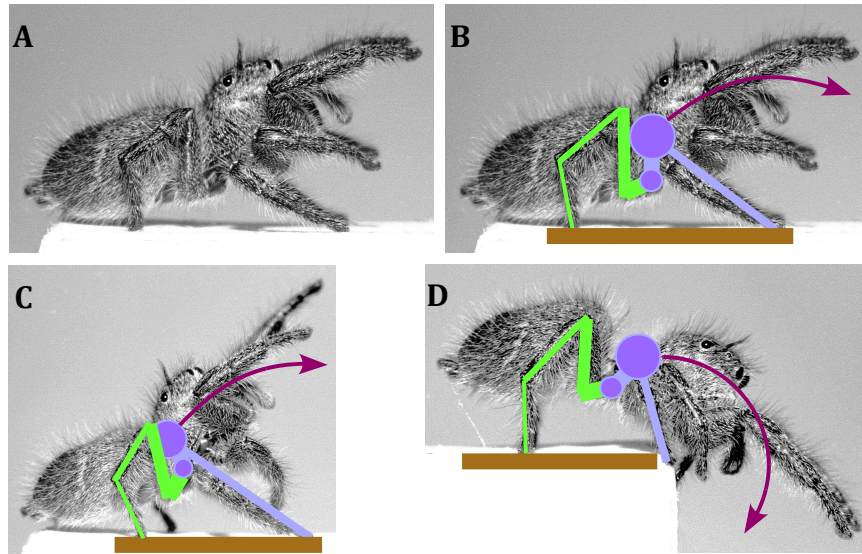
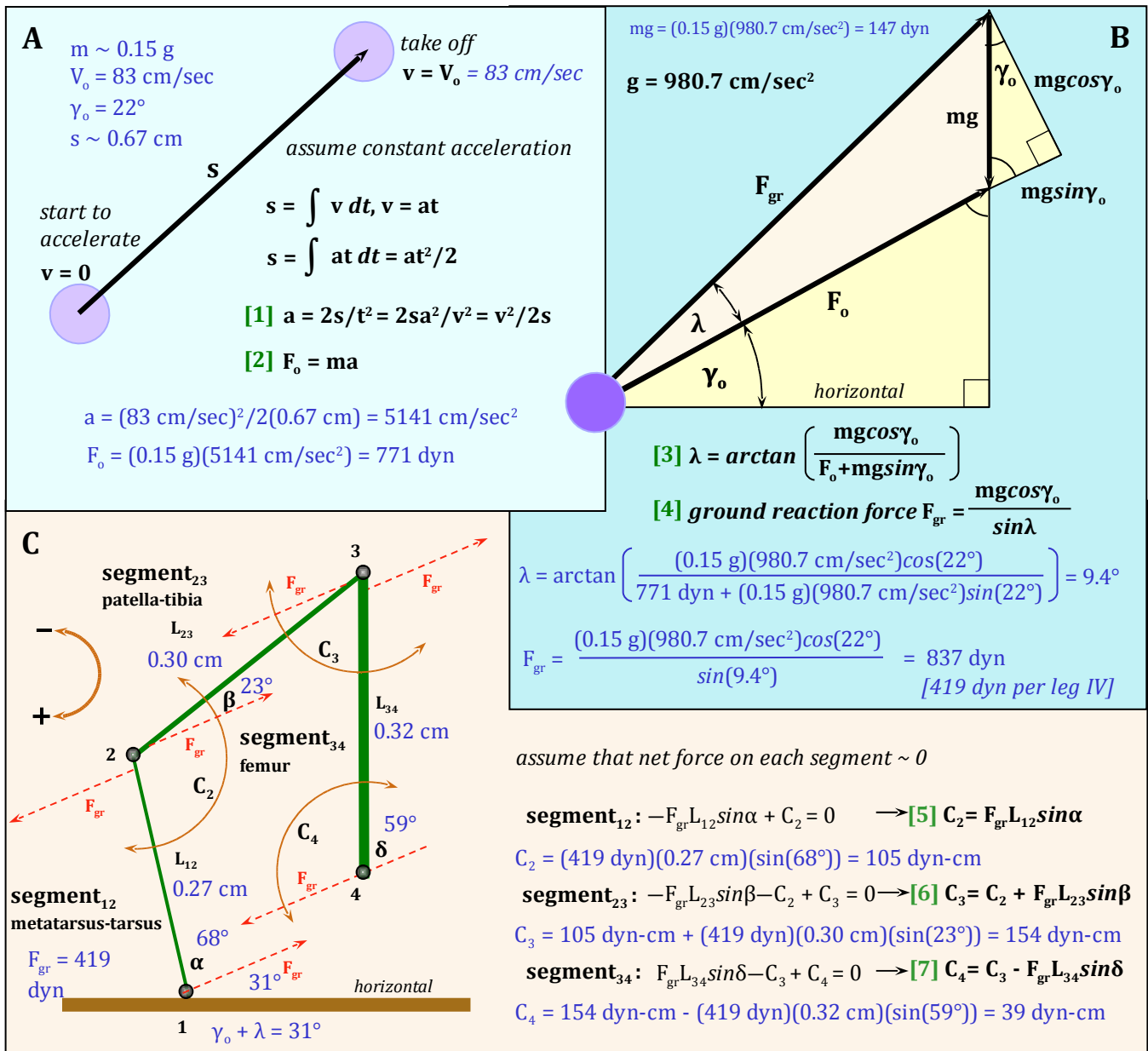


Figure 24 (below). Views of adult female *Phidippus pulcherrimus* from Big Prairie in Ocala National Forest, Florida, preparing to jump. A: On a vertical stem or structure, these spiders would move to a position above the prey in a manner that facilitated their ability to reach that prey. Note that the "stem" in this case was actually a curved surface that the spider would need to accommodate in positioning its legs and steering to jump above the target. In situations like this, the spiders tended to jump sideways, as shown here, and not from a vertical position on the side of the stem facing the target (after Hill 2006a, 2010). B and C: Two views of spiders positioning to make jumps from a positions on a plant. Much versatility was required for these spiders to propel and steer their launch from positions like these, where their exertion (ground force) would cause the plant itself to move backward, and thus lower the substrate resistance required to generate the propulsive ground reaction force. As shown here, *Phidippus* often used both legs II and III to successfully guide or brace a launch from a complex structure. As a spider fed and increased its mass, it also required much more torque to complete its jumps.



Parry and Brown calculated the joint torque that would be required for *Sitticus* to power their jumps with legs IV, and showed that this was consistent with their ability to power take-off through hydraulic extension of legs IV. Their calculations are presented in detail here to make them easier to understand, and similar calculations are also shown for the starting position of *Phidippus princeps* during launch (Figure 25). Note that these calculations are greatly simplified through the assumption that the net force on each leg segment was  $\approx 0$  (actually  $\sim 0$ ), given the relatively small mass of these legs when compared to body mass.

Figure 25. Calculation of torque on joints of leg IV during take off (after Parry and Brown 1959b). Length and mass estimates for adult female *Phidippus princeps* (calculations and measurements highlighted in blue for the starting position of a representative jump) were based on Edwards (2004) and Robertson and Stephens (2002). Other *Phidippus* are much heavier. For example, Lockley and Young (1987) reported a mass of 350 mg for a *P. audax* after it captured and fed on a large cicada. A: Calculation of apparent force at take-off ( $F_o$ ), based on the assumption that acceleration ( $a$ ) is uniform during extension of leg IV over a distance ( $s$ ). Development of the formula for acceleration [1] is shown here. B: Calculation of the ground reaction force ( $F_{gr}$ ) from the apparent force ( $F_o$ ).  $F_{gr}$  is greater because the spider must also counter the opposing force of gravity during acceleration. Note the use of similar triangles (highlighted in yellow) in development of equations [3] and [4]. For Parry and Brown equation [3] was somewhat different, apparently the result of their use of a negative value for  $g$ . Here  $g$  is considered to be positive to avoid any ambiguity. C: Calculation of paired torques (couples) at joints 1, 2, and 3. Each couple ( $C_2, C_3, C_4$ ) represents an equal and opposite torque on joined leg segments in either direction from each joint. A key simplifying assumption is that the net force on each leg segment is equal to 0. This is justified because the mass of the legs is relatively small when compare to the mass of the entire spider, and thus virtually the entire ground reaction force ( $F_{gr}$ ) is driven through the legs to the body. Formulas at the right make use of this assumption in the development of equations [5], [6], and [7], for the three segments shown here. As a convention clockwise torque is positive, and counter-clockwise torque is negative. Parry and Brown used computed torque values to estimate the internal hydraulic pressures that were required to create these torques by means of the formula  $C=k_\theta P$ , where  $C$  was the torque,  $P$  was the internal pressure driving inflation and resultant expansion of the joints, and  $k_\theta$  was a constant for a given joint angle  $\theta$ . Based on earlier work with the agelenid *Tegenaria*, they estimated  $k$  values for *Sitticus*, proportionate to the cube of respective linear hinge dimensions. From the calculation of required hydraulic pressure, they concluded that hydraulic pressure could account for the observed torque.



A comparison of the estimated torque requirements of *Phidippus princeps* with those of *Sitticus pubescens* (Table 1) shows the clear relationship between the much greater mass or weight of *Phidippus* (15 times that of *Sitticus*) and the requirement for much more torque at the leg joints.

Table 1. Comparison of calculated joint torques at take-off for *Sitticus pubescens* (Parry and Brown 1959b) and *Phidippus princeps* (see Figure 25 for calculations). Although the jumps were not identical, the much greater body mass of *P. princeps* was clearly associated with much higher torque values at the hinged joints, by more than an order of magnitude. The length of leg segments in *Sitticus* was proportionately much greater. Salticids vary greatly with respect to *relative* leg length, and *Phidippus* is clearly one of the heavier bodied, *relatively* stocky and shorter legged genera. At the same time, they can deliver a similar rate of acceleration and a similar take-off velocity.

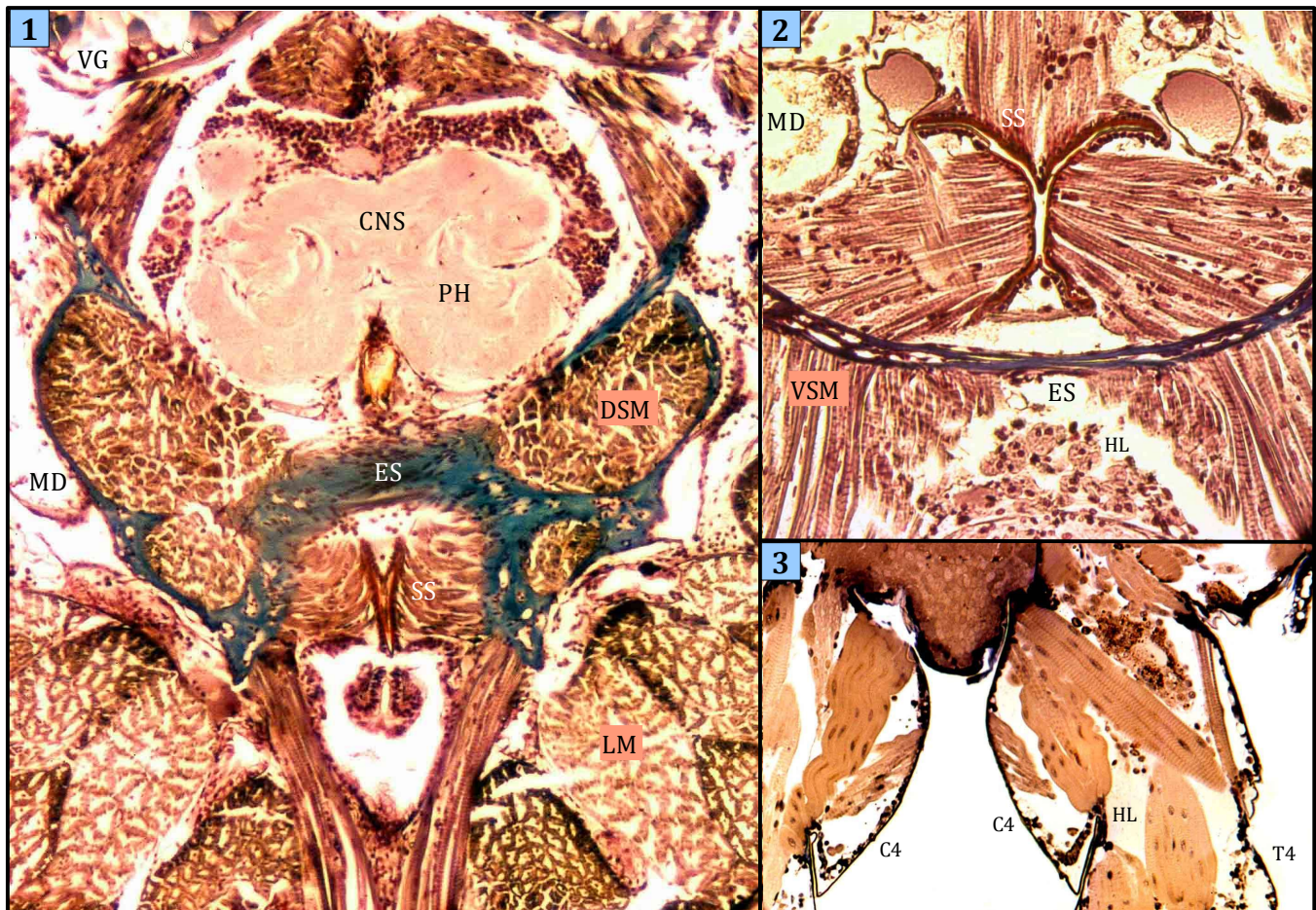
	<i>Sitticus pubescens</i>	<i>Phidippus princeps</i>
mass, m	0.01 g	0.15 g
take off velocity, $V_o$	67 cm/sec	83 cm/sec
take off direction, $\gamma_o$	12°	22°
average acceleration during take off	5130 cm/sec <sup>2</sup>	5141 cm/sec <sup>2</sup>
ground reaction force, $F_{gr}$	55 dyn	837 dyn
length of leg IV patella–tibia, L23	0.22 cm	0.30 cm
direction of ground reaction force (above substratum)	22°	31°
equal and opposite torques (couple) at joint 2, C2	4.8 dyn-cm	105 dyn-cm
equal and opposite torques (couple) at joint 3, C3	6.1 dyn-cm	154 dyn-cm
equal and opposite torques (couple) at joint 4, C4	1.6 dyn-cm	39 dyn-cm

### Hydraulic power

It has long been known that spider leg extension was driven by internal hydraulic pressure (Parry and Brown 1959a, Anderson and Prestwich 1975). In other words, the joints are inflated to extend the legs. More recent studies have also demonstrated a role for elastic energy (generated during flexion of elastic sclerites) in some arachnid joints, but hydraulic pressure still appears to be the primary mechanism behind spider leg extension (Sensenig and Shultz 2003, 2004). As noted by Parry and Brown (1959b), the force that can be generated through the extension of leg segments (inflation of leg joints under pressure) is a factor of the volume of those joints, or the cube of the relative linear dimensions involved. No direct measurements of hydraulic pressures generated by salticids to power these jumps are presently available.

The many large lateral muscles (musculi laterales) of the prosoma were thought to be responsible for generation of this hydraulic pressure, but more recently (Shultz 1991) it has been shown that activity of muscles associated with the endosternite (Figure 26), and not the lateral muscles, is correlated with generation of this pressure.

Figure 26. Internal structures related to the jumping mechanism of *Phidippus* jumping spiders. 1, Horizontal section (Masson Trichrome, 10  $\mu$ m section) through the prosoma of a sixth instar *P. johnsoni*. The anterior direction is toward the top of this photograph. It was thought that the large dorso-ventral, lateral muscles of the prosoma (LM) were responsible for generation of the hydraulic pressure that powers extension of the legs, but more recent evidence suggests that muscles (DSM) attached to the endosternite (ES) are responsible for generation of this pressure in arachnids (Shultz 1991). This view shows the extent of the endosternite as it cradles the "neck" of the central nervous system (CNS) which connects the overlying syncerebrum to the fused leg ganglia, situated below the endosternite and sucking stomach (SS). The endosternite stains like cartilage and is a true, free-floating internal skeletal element of the spider, not involved in the molting process as are the cuticular plates that line the pharynx (PH) and sucking stomach (SS). This ability to move within the prosoma may play an important role with respect to the generation of high internal fluid pressure by the endosternite. 2, Transverse section (Masson Trichrome, 10  $\mu$ m section) through the prosoma of a sixth instar *P. johnsoni*. Note the large ventral muscles (VSM) attached to the endosternite, and the hemolymph space (HL, near several large binucleate cells) directly below the endosternite, just above the central nervous system (CNS). This view also provides a good view of the powerful transverse musculature responsible for generation of vacuum pressure in the sucking stomach (SS, at center). Comparing this view with (A), you should be able to see how the sucking stomach is cradled within the endosternite, and also anchored to it with many powerful muscles that pull the stomach plates apart to create vacuum pressure. 3, Section (Toluidine Blue, 5  $\mu$ m Epon section) through the coxae of legs IV (C4) of a second instar *P. johnsoni*. Note the large hemolymph (HL) spaces in the legs between the muscles. Abbreviations used are: C4 coxa of leg IV, CNS central nervous system, DSM dorsal muscles attached to the endosternite, ES endosternite, HL hemolymph space, LM lateral muscles (dorso-ventral) of the prosoma, MD midgut diverticulum, SS sucking stomach, PH pharynx or rigid feeding tube that passes through the central nervous system and conveys food to the sucking stomach, T4 trochanter of leg IV, VG venom gland, and VSM ventral muscles attached to the endosternite.



### *Pitch and roll during ballistic flight*

As shown here, *backward pitch* is a regular feature of salticid flight. Attachment of legs IV below the center of gravity of the spider facilitates this through the generation of torque on the center of gravity/articulation couple. Backward pitch clearly plays an important role in positioning the spider for its attack on the prey.

The *roll* that has been observed is also important in that in certain circumstances it allows these spiders to move to a horizontal position above the target, at the point of attack. This horizontal orientation during flight appears to be the preferred orientation, regardless of the orientation of the launch substratum. To effect this roll from a vertical surface that lies in the plane of attack, the spider must exert more force against the substratum on its lower side during take off, thus producing the required torque as part of the ground reaction force. This must be accomplished prior to ballistic flight, through positioning and application of the limbs against the substratum.

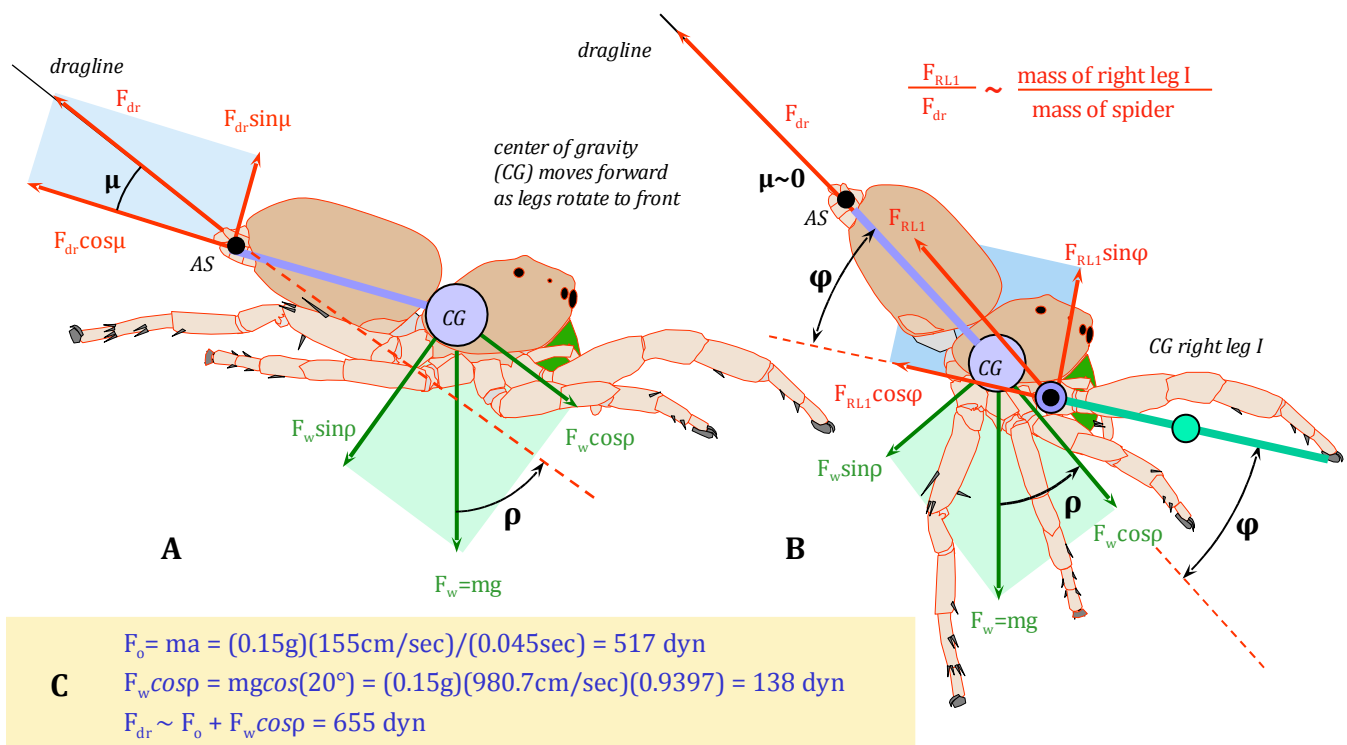
Once launched into ballistic flight, the spider can and does move its limbs relative to its body, but it cannot alter the total angular momentum of its body, as generated by torque during take off and represented by its pitch and roll (angular velocities  $\omega_P$  and  $\omega_R$ , respectively) during the early part of flight, until it brakes on the dragline.

### *Braking on the dragline*

As shown in Figure 20, *Phidippus* (and presumably other salticids) generally jump with a secured dragline. One exception to this can be readily observed when you try to catch these spiders in the field and they drop quickly through the vegetation, demonstrating that they are able to release the dragline quickly. Similar *free-fall* behavior can be observed when they are approached by a wasp. During longer jumps, *Phidippus* usually brake on the dragline, reversing the pitch, apparently near a precalculated target distance. In many if not most situations, the prey is not in the field of vision of these spiders when braking takes place. Braking is associated with the continued forward movement of all eight legs, which collectively form a "catching basket" of spiny legs that entraps the prey. A dangling salticid is relatively safe as a large prey item struggles in its grasp, since that prey has no recourse to ground force. Braking on the dragline must be responsible for both deceleration and reversal of pitch in flight, as there is no other agent present to effect these. Parry and Brown (1959b) noted this likely relationship, and they also saw a *Sitticus* make a complete somersault at the end of a jump when it appeared that its dragline was broken.

An analysis of torque related to dragline braking and reversal of pitch is presented in Figure 27. Once braking begins, momentum pulls the limbs of the spider together as they form a catching basket. This analysis is not meant to suggest that active muscular flexion of the legs is not taking place at the same time, and I would assume that it is. Torque does support this movement, nonetheless. As braking is completed, the force of gravity is converted into torque at the falling spider end of a spider/dragline pendulum. The other (radial or dragline-parallel) component of gravity is completely countered by the dragline ground reaction at that time. As a result, the falling spider can be seen to accelerate in the same manner as a pendulum, until it has fallen as far as the dragline will permit.

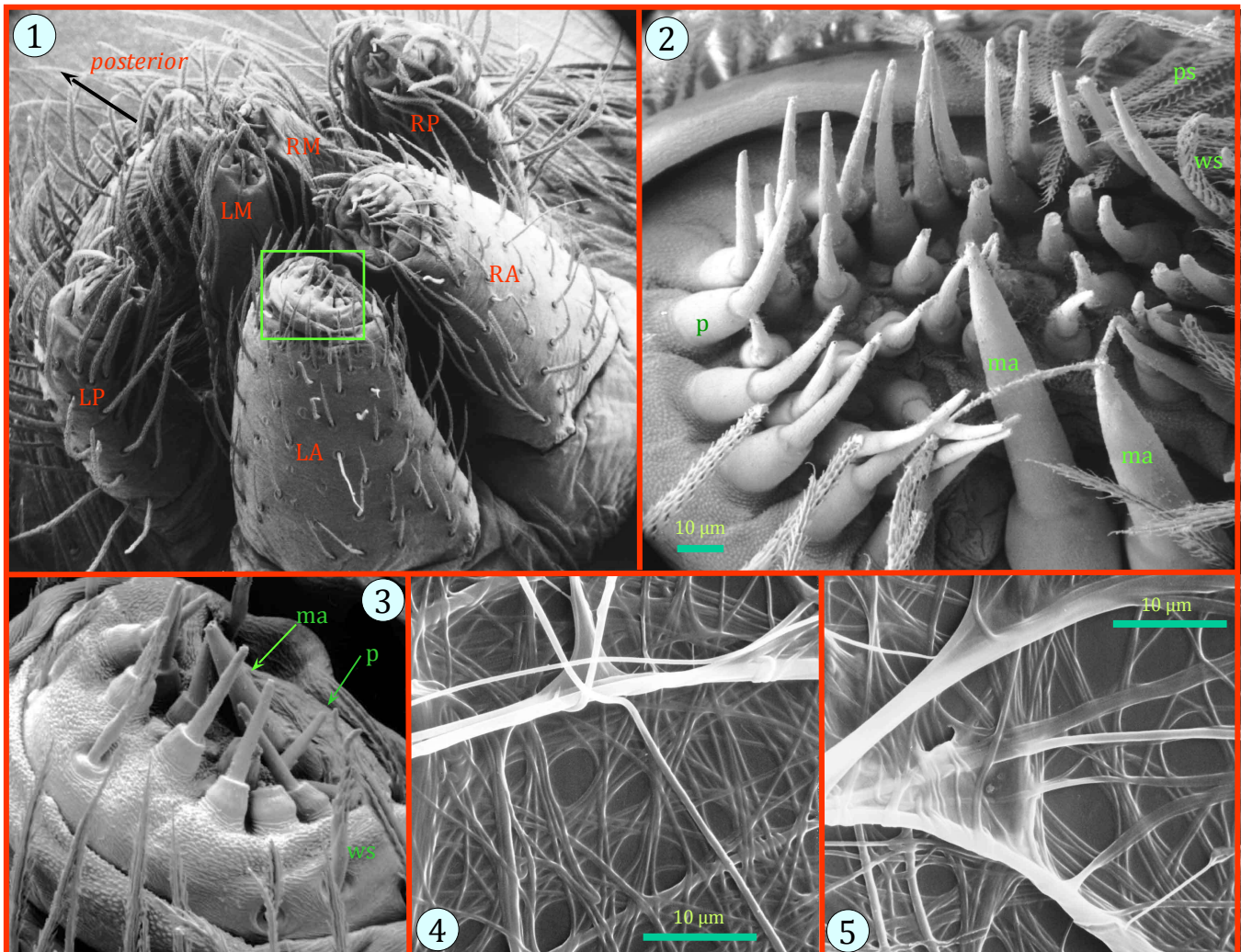
Figure 27. Impact of dragline reaction force on the orientation of *Phidippus* during flight. Just as ground reaction force represents the equal and opposite reaction to the spider's push against the substratum, dragline reaction force represents the equal and opposite reaction to dragline force (pull) exerted by the spider on the dragline as it brakes. During braking, dragline force essentially represents conversion of the linear momentum of the spider in flight to the dragline. A: At the onset of the braking cycle, the spider's grip on the dragline (at the anterior lateral spinnerets, AS) and its center of gravity (CG) form a couple between the forces of gravity ( $F_w$ ) and dragline reaction ( $F_{dr}$ ), due to the offset ( $\mu$ ) between the long axis of the spider and the dragline vector. Thus the dragline reaction has both braking ( $F_{dr}\cos\mu$ ) and angular acceleration ( $F_{dr}\sin\mu$ , driving forward angular acceleration and pitch) components. To slow down the spider ( $F_o$  or observed deceleration force  $>0$ ), the dragline reaction force has to be greater than the opposing force of gravity ( $\sim F_w \cos\rho$ , where  $\rho$  is the inclination of the long axis of the spider with respect to a vertical plane). The force of gravity ( $F_w$ ) can be separated into this component that opposes dragline braking ( $F_w \cos\mu$ ), and a tangential component ( $F_w \sin\mu$ ) that accelerates the center of gravity of the spider around the dragline attachment disk as it continues to fall as a pendulum. B: Later in the jump, the long axis of the spider (AS–CG) is aligned with the dragline and the dragline reaction force. As shown here, as long as leg I (or any other leg) is out of alignment with the long axis (angle  $\phi$ ), a component of the dragline reaction force ( $F_{RL1}$ , representing the mass-proportionate allocation of that force to right leg I) will drive that leg toward the center axis of the spider with a force  $F_{RL1}\sin\phi$  (drawn out of scale here). The center of gravity of right leg I is approximated with a green circle. This angular acceleration relative to the body is not countered by gravity, which affects all parts of the spider with the same acceleration, so it may be quite significant. Powerful flexor muscles in the legs may also play a key role in their rapid movement during the grasp, and they continue to play a major role as struggling prey is held securely and subdued. C: Calculation of forces related to dragline deceleration based on a real example where the spider was dropping at about 150 cm/sec at a  $-70^\circ$  inclination ( $\rho=20^\circ$ ). An estimate of adult female *P. princeps* mass based on Edwards (2004) and Robertson and Stephens (2002) was used. The spider braked to a complete stop in the direction of movement within 45 msec (0.045 sec). With the assumption of uniform deceleration, the net force  $F_o$  was approximately 517 dyn, as shown here. Given the need to counter 138 dyn of gravitational force to effect this deceleration, the actual dragline reaction force ( $F_{dr}$ ) was closer to 655 dyn. In some cases this very significant force may be even greater than the ground reaction force during take off. The assumption of uniform deceleration used in this calculation is useful but it is not accurate, and observation of jump photographs suggests that in many cases slower braking associated with alignment of the body and legs precedes a sudden impulse at the point of attack with much greater force over a short time interval. Collision with prey of any size would also be a significant factor affecting the trajectory of a spider. Stretching by the elastic dragline when it is subjected to force is also an important factor that greatly impacts the dynamics of braking by temporarily lowering resistance as well as the dragline reaction force. Since the mass of the dragline itself is negligible, the ability to pull (apply force to) the substratum through the dragline attachment disk is critical to creation of the opposing dragline reaction force, and elasticity of the dragline temporarily reduces this ability.



### The dragline

Salticids, like other spiders, are masters in the production and use of silk lines. The dragline represents the most constant use of silk by these spiders, and as shown here, plays a key role in their jumps. As shown in Figure 28, the dragline of *Phidippus* is produced from two large spigots associated with each of the anterior lateral spinnerets. Each spigot is associated with one of the four large ampullate glands of the spider. Also associated with the anterior lateral spinnerets are many smaller spigots, each associated with a small pyriform gland. These are responsible for the creation of the attachment disk (Figure 28D, E) that secures the dragline to the substratum (Kovoor 1987, Moon 2006).

Figure 28. SEM views of the silk and spinnerets of *Phidippus audax* from Iowa City, Iowa. 1, Ventral view of spinnerets of an immature *P. audax*. Anterior spinnerets (LA and RA) are responsible for production and release of both dragline and attachment disk silk. 2, Right anterior spinneret of an adult female *P. audax*. Both of the two major ampullate spigots (ma) associated with this spinneret can be seen in this view. Note the large number of smaller spigots associated with pyriform glands (p). Both chemosensory whorled setae (ws) and plume setae (ps) are associated with the spinnerets. Both kinds of setae are also found on the tarsus and pretarsus of each leg (Hill 1977b). Plume setae are thought to be associated with rapid silk handling. 3, Detail from (1) of spigots associated with left anterior spinneret. One large spigot (MA or major ampullate) is visible in this view. This spigot is associated with one of the four major ampullate glands and production of the dragline. The many smaller spigots (P) are associated with the small pyriform glands. They produce the many smaller strands of silk that comprise the attachment disk. 4–5, Two views of dragline silk (larger fibers free of surface) and its relationship to attachment disk silk, produced by a penultimate female *P. audax*. These attachment disks were deposited on a smooth plastic surface. Note the extruded and flattened appearance of the many smaller diameter fibers of the attachment disk, and their adhesion to the larger dragline fibers. Abbreviations: LA and RA: left and right anterior (lateral) spinnerets, LM and RM: left and right (posterior) medial spinnerets, LP and RP: left and right posterior (lateral) spinnerets, ma: spigots of the major ampullate (dragline) glands, p: spigots of the pyriform (attachment disk) glands, ws: whorled or chemosensory seta, ps: plume setae.



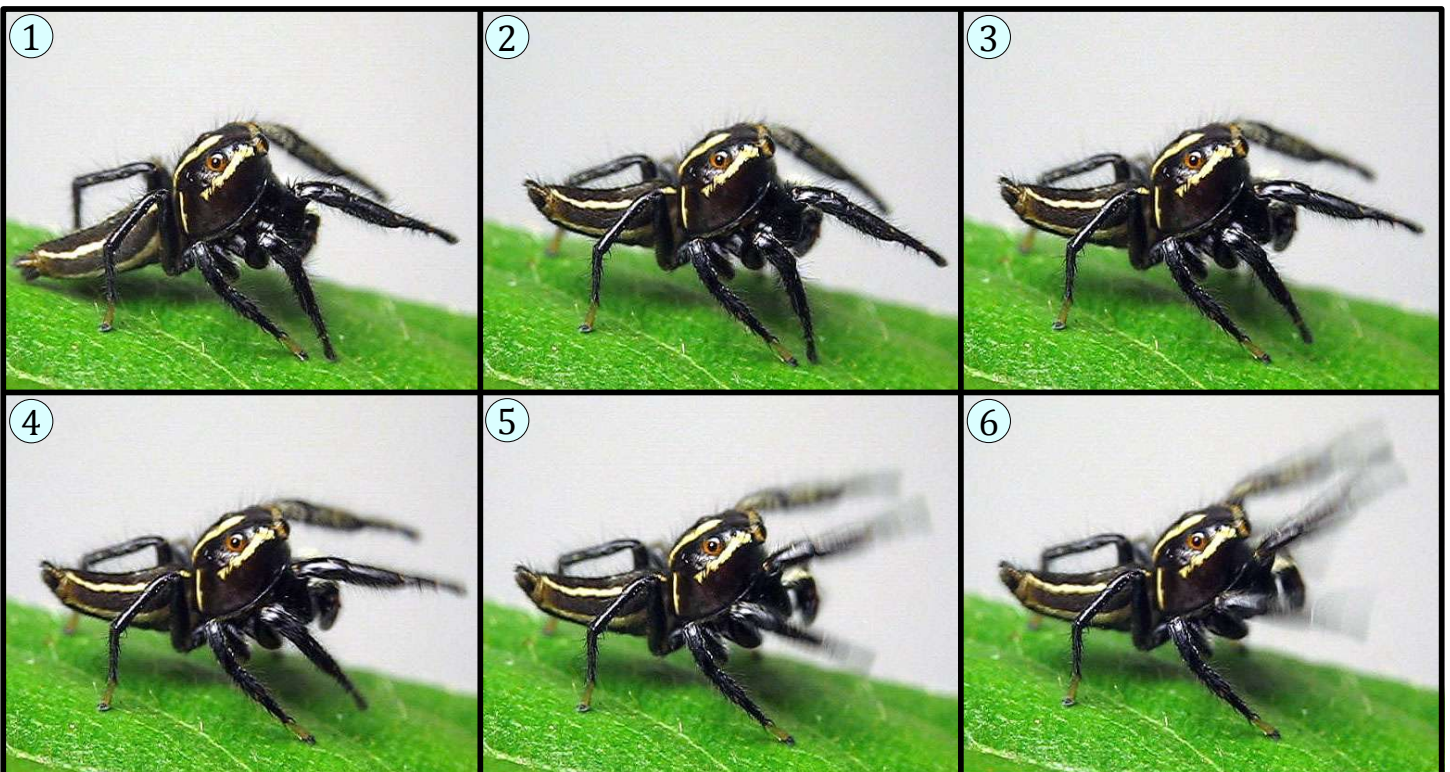
Work (1978) proposed that dragline braking might be accomplished by pulling the respective spinnerets together thus engaging the drawn fibers. The most widely accepted view at the present time is that valves and associated muscles at the base of each spigot are responsible for this braking (e.g., Vollrath and Knight 2001, Saravanan 2006).

Most study of dragline silk, or the silk produced by the major ampullate (MA) glands of spiders, has been based on the study of araneid (orb-weaving) spiders (e.g., Xu and Lewis 1990, Gosline *et al.* 2001). Araneids use this silk for draglines, but they also use it to create the structural framework of their orb webs. Through a complex internal structure that combines crystalline components with long polymer chains, dragline fibers possess a unique and remarkable combination of strength and elasticity. Gosline *et al.* (1999) reported extensibility (elasticity) of 0.27 (27%) for the dragline silk of the araneid *Araneus*, but also described its strength as follows: *It is fair to say that spider MA silk is among the stiffest and strongest polymeric biomaterials known.* As much as 65% of the kinetic energy associated with stretching of araneid MA fibers is converted into heat and not into elastic recoil (Gosline *et al.* 1999). It is likely that similar properties associated with salticid dragline silk contribute to the smooth pendulum movement of these animals at the end of a long predatory jump, as the elastic dragline absorbs some of the recoil from the pull of the spider (dragline force) and converts this into heat and ground force applied at the attachment disk. When not stretching, dragline tension is the result of the equal and opposite dragline force (at the spider end) and ground reaction force (at the attachment disk end).

#### *The catching basket*

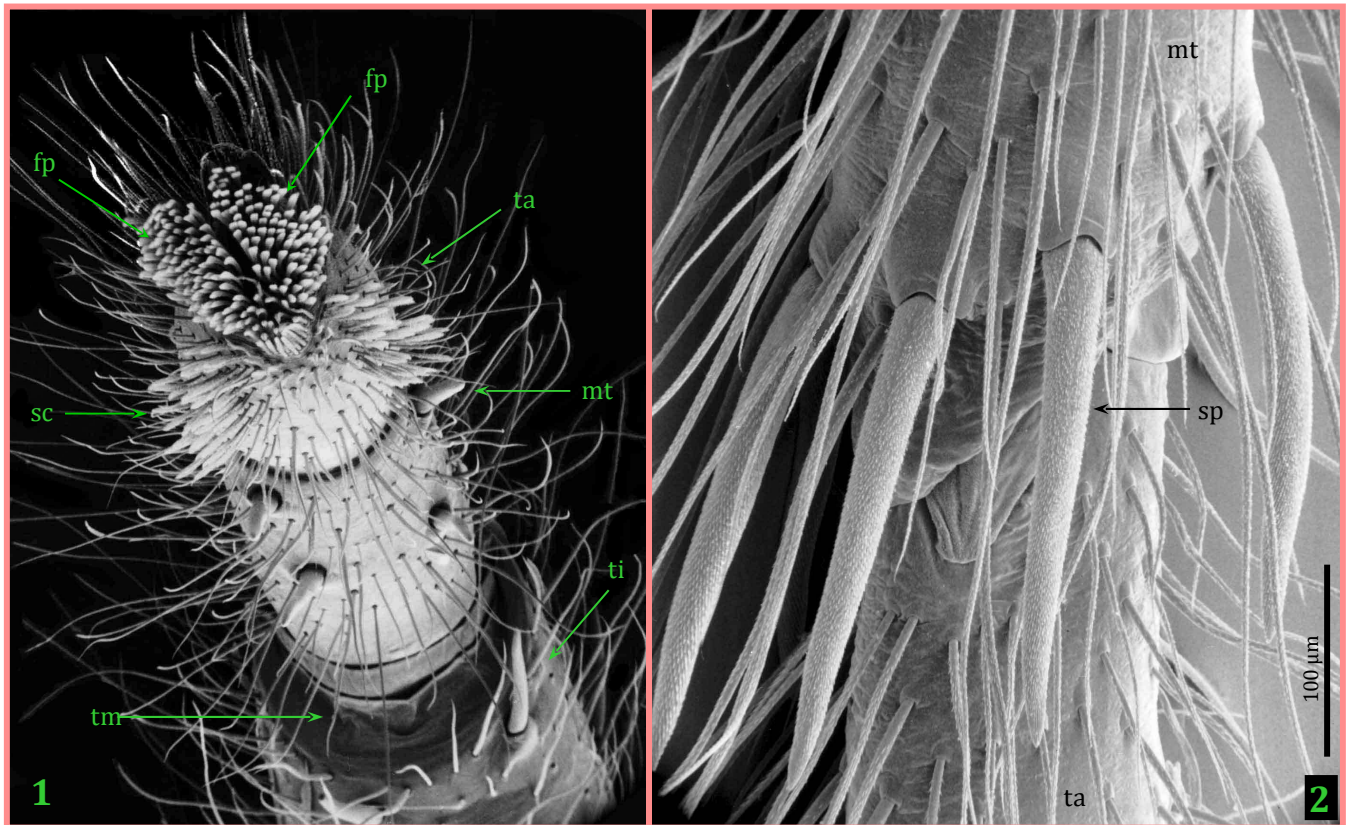
Salticid spiders are generally armed with stout spines that can assist in the capture and handling of prey. In general, legs I and II are extended prior to execution of a jump, presenting spines on the underside of these legs in the direction of a target (Figure 29).

Figure 29. Sequential frames (1–6) from video clip of a jumping adult male *Thiodina puerpera* (Hentz 1846) from Greenville County, South Carolina. 1, Spinnerets move up and down to produce attachment disk. 2, Opisthosoma raised to prepare for jump. 3, Legs II lifted off of the leaf. 4–5, Legs I and II raised. 6, Final position about 1/60 s before launch. In all aspects the jumping posture of this amycooid salticid compared to that of the marpissoid *Phidippus*, although the two species are distant relatives within the Neotropical Salticoida (Maddison and Hedin 2003).



All of the legs of *Phidippus* are armed with these spines, particularly on the inward surface of the distal segments (Figure 30). These surround the prey as the legs are pulled together in flight to form a *catching basket*. The emphasis on development of strong muscular flexion in the legs of spiders contributes to the strength of this attack. Movement and use of the chelicerae and fangs has not been observed directly during these attacks, but as soon as the prey has been grasped, their use can be observed (see also Figure 1).

Figure 30. SEM photographs of prominent leg spines of *Phidippus audax* (Hentz 1845) from Iowa City, Iowa. 1, Inside view of the distal portion of leg I. Note the four large spines on the inside (catching basket) side of the metatarsus (mt), and two of the spines associated with the inside of the tibia (ti). The tarsus (ta) has both anterior and posterior scopulae (sc) comprised of lamelliform tenent setae (tenae). The anterior and posterior foot pads (fp) are also comprised of tenent setae (ts) associated with pretarsal plates that can be extended or retracted relative to the tarsus (Hill 2006b). The two claws are behind the tenent setae and are not visible in this view. The flexible and expandable ventral margin of the tibio–metatarsal joint (tm) can also be seen in this view. 2, View of the metatarsus (mt) and tarsus (ta) of the left leg IV of an adult male. Prominent spurs (sp) attached to the distal metatarsus form part of the catching basket. The joint between the metatarsus and the tarsus (center) provides useful but limited flexibility.



### Acknowledgments

This work was initiated more than 27 years ago (1978), when I was a postdoctoral associate in the Department of Neurobiology and Behavior at Cornell University. Results have been recomputed several times in the intervening years, based on the availability of more advanced computing technology and improved algorithms. Related studies were initiated as part of my graduate work at Oregon State University (1973–1975), the University of Iowa (1975–1976), and the University of Florida (1976–1978). I thank Dr. Thomas Eisner of Cornell University for his strong support for this, and related, work at Cornell University. I would also like to thank Dr. C. J. Bayne, Dr. Bruce Cutler, Dr. G. B. Edwards, Dr. Jonathan Reiskind, Dr. David Richman, and Dr. C. Y. Shih for their respective support during the development of this work. The specific subject of this study was originally suggested by G. B. Edwards.

## References

- Anderson, J. F., and Prestwich, K. N. 1975.** The fluid pressure pumps of spiders (Chelicerata, Araneae). *Zeitschrift für Morphologie der Tiere* 81: 257–277.
- Edwards, G. B. 2004.** Revision of the jumping spiders of the genus *Phidippus* (Araneae: Salticidae). *Occasional Papers of the Florida State Collection of Arthropods* 11: i–viii, 1–156.
- Gosline, J. M., P. A. Guerette, C. S. Ortlepp and K. N. Savage. 1999.** The mechanical design of spider silks: from fibroin sequence to mechanical function. *The Journal of Experimental Biology* 202: 3295–3303.
- Hill, D. E. 1977a.** Field observations on the behavior of immature *Phidippus princeps* in Minnesota. *Peckhamia* 1(3): 44–50.
- Hill, D. E. 1977b.** The pretarsus of salticid spiders. *Zoological Journal of the Linnean Society, London* 60 (4): 319–338.
- Hill, D. E. 1978.** Orientation by jumping spiders of the genus *Phidippus* (Araneae: Salticidae) during the pursuit of prey. PhD. Dissertation, University of Florida, i–v, 1–202.
- Hill, D. E. 1979.** Orientation by jumping spiders of the genus *Phidippus* (Araneae: Salticidae) during the pursuit of prey. *Behavioral Ecology and Sociobiology* 6: 301–322.
- Hill, D. E. 2006a.** Use of location (relative direction and distance) information by jumping spiders (Araneae, Salticidae, *Phidippus*) during movement toward prey and other sighted objectives. *Version 2*: 1–72.
- Hill, D. E. 2006b.** Jumping spider feet (Araneae, Salticidae). *Version 3*: 1–41.
- Hill, D. E. 2009.** Euophryine jumping spiders that extend their third legs during courtship (Araneae: Salticidae: Euophryinae: *Maratus, Saitis*). *Peckhamia* 74.1: 1–27.
- Hill, D. E. 2010.** Use of location (relative direction and distance) information by jumping spiders (Araneae, Salticidae, *Phidippus*) during movement toward prey and other sighted objectives. *Peckhamia* 83.1: 1–103.
- Kovoor, J. 1987.** Comparative structure and histochemistry of silk-producing organs in arachnids. In: Nentwig, W. (ed.) *Ecobiology of Spiders*, Springer-Verlag, Berlin: 159–186.
- Lockley, T. C., and O. P. Young. 1987.** *Phidippus audax* (Araneae, Salticidae) predation upon a cicada (*Tibicen* sp.) (Homoptera, Cicadidae). *Journal of Arachnology* 14: 393–394.
- Maddison, W. P. and M. C. Hedin. 2003.** Jumping spider phylogeny (Araneae: Salticidae). *Invertebrate Systematics* 17: 529–549.
- Moon, M.-J. 2006.** Microstructure of the silk-spinning nozzles in the lynx spider, *Oxyopes licenti* (Araneae: Oxyopidae). *Integrative Biosciences* 10: 85–91.
- Otto, J. and D. E. Hill. 2010a.** Observations of courtship display by a male *Maratus amabilis* Karsch 1878 (Araneae: Salticidae). *Peckhamia* 79.1: 1–16.
- Parry, D. A., and R. H. J. Brown. 1959a.** The hydraulic mechanism of the spider leg. *Journal of Experimental Biology* 36: 423–433.
- Parry, D. A., and R. H. J. Brown. 1959b.** The jumping mechanism of salticid spiders. *Journal of Experimental Biology* 36 (4): 654–664.
- Robertson, M. W., and A. Stephens. 2002.** Mating behavior, reproductive biology, and development of *Phidippus princeps* (Araneae: Salticidae). *Transactions of the Illinois State Academy of Science* 95 (4): 335–345.
- Robinson, M. H., and C. E. Valerio. 1977.** Attacks on large or heavily defended prey by tropical salticid spiders. *Psyche*, Cambridge 84 (1): 1–10.
- Saravanan, D. 2006.** Spider silk – structure, properties, and spinning. *Journal of Textile and Apparel, Technology and Management* 5 (1): 1–20.
- Sensenig, A. T., and J. W. Shultz. 2003.** Mechanisms of cuticular elastic energy storage in leg joints lacking extensor muscles in arachnids. *Journal of Experimental Biology* 206: 771–784.
- Sensenig, A. T., and J. W. Shultz. 2004.** Elastic energy storage in the pedipalpal joints of scorpions and sun-spiders (Arachnida, Scorpiones, Solifugae). *The Journal of Arachnology* 32: 1–10.
- Shultz, J. W. 1991.** Evolution of locomotion in Arachnida: the hydraulic pressure pump of the giant whipscorpion *Mastigoproctus giganteus* (Uropygi). *Journal of Morphology* 210: 13–31.
- Vollrath, F. and D. P. Knight. 2001.** Liquid crystalline spinning of spider silk. *Nature* 410: 541–548.
- Waldock, J. M. 2007.** What's in a name? Or: why *Maratus volans* (Salticidae) cannot fly. Western Australian Museum. [http://www.australasian-arachnology.org/download/Maratus\\_cannot\\_fly.pdf](http://www.australasian-arachnology.org/download/Maratus_cannot_fly.pdf)
- Waldock, J. M. 2008.** Debunking an urban myth: The jumping spider *Maratus* cannot fly. Australasian Arachnological Society. [http://www.australasian-arachnology.org/myths/maratus\\_cannot\\_fly/](http://www.australasian-arachnology.org/myths/maratus_cannot_fly/)
- Work, Robert W. 1978.** Mechanisms for the deceleration and support of spiders on draglines. *Transactions of the American Microscopical Society* 97 (2): 180–191.
- Xu, M. and R. V. Lewis. 1990.** Structure of a protein superfiber: spider dragline silk. *Proceedings of the National Academy of Sciences, USA* 87: 7120–7124.

## Appendix 1. Program used to compute take off velocity and direction

This C program was originally written and compiled for Apple Macintosh<sup>(TM)</sup> computer, but it could also be compiled on other platforms if linked to appropriate source libraries. This is a successive approximation program used to calculate the magnitude of the take off velocity ( $V_0$ ) and the take off direction relative to a horizontal plane ( $\gamma_0$ ) from two input positions of the spider center of gravity in flight ( $X1, Y1$  and  $X2, Y2$  respectively, corresponding to positions C and D in Figures 3 and 4), as measured from the reference origin (0,0 corresponding to position A in Figures 3 and 4). This program "walks" up the parabola of the flight trajectory in increments until it crosses the radius of the take-off circle, then moves back along the computed trajectory until outside of that circle in smaller increments, and then reverses again in yet smaller increments. This is repeated until the intersection of the take-off circle (radius) and flight trajectory is determined to a high degree of accuracy. The take off velocity ( $V_0$  and  $\gamma_0$  components) is then computed for this position. This algorithm is useful because it converges rapidly in all cases, even when jumps are near vertical. This successive approximation method is explained in more detail in the text. Only the blue lines shown here are compiled and executable. The red lines are comments.

```

#include <stdio.h> #include <math.h>
main()
{
/*DECLARATION OF VARIABLES*/
/*interval between images in milliseconds*/
/*take off radius in centimeters*/
/*input coordinates in cm at 3x scale*/
/*corrected coordinates in cm at 1x*/
/*g in cm/sec/sec*/
/* take off vx, vy in cm/sec, vy at y1*/
/*x and y coordinates at take off*/
/*approximation for y0*/
/*time after take off at (x1,y1)*/
/*take off direction in degrees*/
/*take off velocity in cm/sec*/

double interval;
double radius;
double input_x1,input_y1,input_x2,input_y2;
double x1,y1,x2,y2;
double gravity = 980.7;
double vx0,vy0,vy1;
double x0,y0;
double y0a;
double time;
double direction;
double velocity;
double pi = 3.14159; int counter;

/*USER PROMPTS FOR REFERENCE DATA*/
/*user prompted for interval between pictures*/

printf("enter interval in msec (e.g., 15.00):"); scanf("%lf",&interval);
interval=interval/1000;
printf("enter radius in mm (e.g., 6.7 or 10.0):");
scanf("%lf",&radius); radius=radius/10;
printf("\n"); printf("\n");

/*user prompted for radius of take off circle */

/*ITERATIVE LOOP FOR MULTIPLE DATA SETS*/
/*maintains loop for successive iterations*/

while (pi>0)
{
/*INPUT OF MEASURED POSITIONS RECORDED FROM 3X SCALE PHOTOGRAPHS */
printf("enter x1:"); scanf("%lf",&input_x1); printf("enter x2:"); scanf("%lf",&input_x2);
printf("enter y1:"); scanf("%lf",&input_y1); printf("enter y2:"); scanf("%lf",&input_y2);
printf("\n");

/*SCALE CORRECTION AND INITIAL CALCS*/

x1=input_x1/3;y1=input_y1/3;
x2=input_x2/3;y2=input_y2/3;
vy1=((y2-y1)/interval) + 0.5 * gravity * interval;
vx0=(x2-x1)/interval;

/*NESTED SUCCESSIVE APPROXIMATION LOOP TO FIND TAKE OFF POSITION */
/*starting values for successive approximation*/
x0=x1; y0=y1;
/*series of loops with increasing resolution*/
while ((sqrt(x0*x0+y0*y0))>radius) {x0 = x0-0.1; time = (x1 - x0)/vx0; y0 = y1 - vy1*time -0.5*gravity*time*time;}
while ((sqrt(x0*x0+y0*y0))<radius) { x0 = x0+0.01; time = (x1 - x0)/vx0; y0 = y1 - vy1*time -0.5*gravity*time*time;}
while ((sqrt(x0*x0+y0*y0))>radius) { x0 = x0-0.001; time = (x1 - x0)/vx0; y0 = y1 - vy1*time -0.5*gravity*time*time;}
while ((sqrt(x0*x0+y0*y0))<radius) {x0 = x0+0.0001; time = (x1 - x0)/vx0; y0 = y1 - vy1*time -0.5*gravity*time*time;}
while ((sqrt(x0*x0+y0*y0))>radius) {x0 = x0-0.00001; time = (x1 - x0)/vx0; y0 = y1 - vy1*time -0.5*gravity*time*time;}
while ((sqrt(x0*x0+y0*y0))<radius) {x0 = x0+0.000001; time = (x1 - x0)/vx0; y0 = y1 - vy1*time -0.5*gravity*time*time;}
while ((sqrt(x0*x0+y0*y0))>radius) {x0 = x0-0.0000001; time = (x1 - x0)/vx0; y0 = y1 - vy1*time -0.5*gravity*time*time;}

/*FINAL CALCULATIONS AND OUTPUT BASED ON KNOWN TAKE OFF POSITION*/
vy0 = vy1 + gravity*time;
direction = atan(vy0/vx0) * (180/pi);
velocity = sqrt (vx0*vx0 + vy0*vy0);
printf("starting x in cm = %f \n", x0); printf("starting y in cm = %f \n", y0);
printf("radius in cm = %f \n", sqrt(x0*x0+y0*y0));
printf("(x1,y1) time in sec = %f \n", time); printf("take off vx in cm/sec = %f \n", vx0);
printf("take off vy in cm/sec = %f \n", vy0);
printf("\n"); printf("velocity in cm/sec = %f \n", velocity);
printf("direction in degrees = %f \n", direction);
printf("\n"); printf("\n"); }

/*THIS PROGRAM LOOPS BACK FOR DATA AND WILL NOT STOP UNTIL INTERRUPTED*/
}

```

## Appendix 2. Maximum horizontal range as function of take off velocity

There have been many claims of long jumps by salticid spiders, with little documentation. This chart is provided as a quick reference for estimation of take off velocity ( $V_0$ ) from the maximum horizontal range ( $S_x$ ) of a jump. With a series of photographs or frames from video of salticids jumping on a horizontal surface, these measurements should be easy to obtain for species that have not otherwise been studied.

Documented take off velocities for several jumping spiders have been in the 50–100 cm/s range (shaded area below) The maximum horizontal range assumes a take-off direction of  $45^\circ$  above the horizontal, and this is not necessarily the fastest jump that a salticid can make to a targeted position. Many arthropods greatly exceed the jumping velocities of salticid spiders, but accuracy is generally far more important than range for these spiders as they jump toward sighted objectives.

